PTA and Cyclohexyl Groups Impart to Di-Iron(I) Complex Aqueous Solubility and Stability, and Prominent Anticancer Activity in Cellular and Animal Models

Michele De Franco,[a] Lorenzo Biancalana,[b,*] Chiara Zappelli,[b] Stefano Zacchini [c]
Valentina Gandin,[a,*] Fabio Marchetti [b,*]

[b] University of Padova, Department of Pharmaceutical and Pharmacological Sciences, Via F. Marzolo 5, I-35131 Padova, Italy.

[b] University of Pisa, Department of Chemistry and Industrial Chemistry, Via G. Moruzzi 13, I-56124 Pisa, Italy.

[c] University of Bologna, Department of Industrial Chemistry "Toso Montanari", Via P. Gobetti 85, I-40129 Bologna, Italy

lorenzo.biancalana@unipi.it, valentina.gandin@unipd.it, fabio.marchetti@unipi.it

Supporting Information

Table of contents **Page(s)**

Structures of diiron complexes (**Charts S1-S9**) S2-S3
IR, NMR and ESI-MS spectra of diiron compounds (**Figures S1-S46**) S4-S26
Thermal isomerization in isopropanol (**Figures S47-S50**) S27-S28
Comparison of selected NMR and IR data (**Tables S1-S2**) S29-S30
Behavior of the diiron complexes in aqueous solutions (**Tables S3-S5**) S31-S36
Cyclic voltammetry (**Figure S51**) S37
X-ray crystallography (**Table S6**) S38
In vivo biological studies S39
Notes and references S40

Chart S1. Structure of the cation within **2a** (numbering refers to C atoms; wavy bonds refer to *E*/*Z* isomerism).

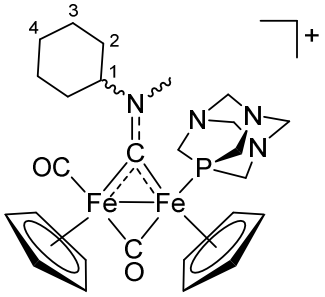

Chart S2. Structure of the cation within **2b** (numbering refers to C atoms; wavy bonds refer to *E*/*Z* isomerism).

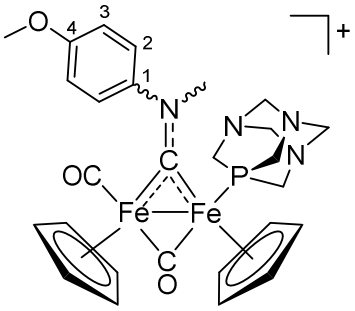

Chart S3. Structure of the cation within **2c** (numbering refers to C atoms; wavy bonds refer to *E*/*Z* isomerism).

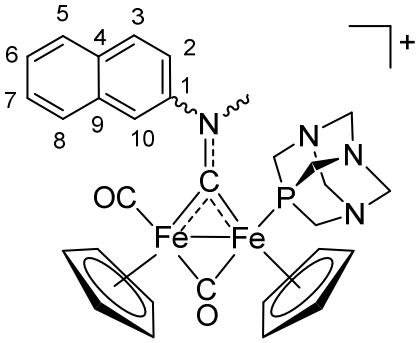

Chart S4. Structure of the cation within **2d** (numbering refers to C atoms; wavy bonds refer to *cis*/*trans* isomerism).

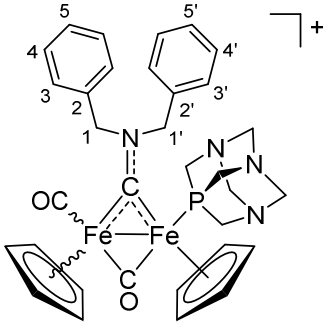

Chart S5. Structure of the cation within **2e** (numbering refers to C atoms; wavy bonds refer to *E*/*Z* isomerism).

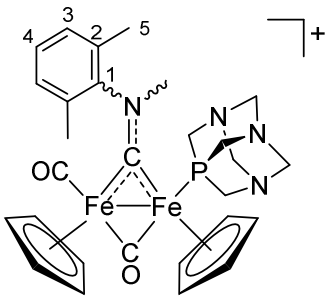

Chart S6. Structure of the cation within **3c** (numbering refers to C atoms; wavy bonds refer to *cis*/*trans* and *E*/*Z* isomerism).

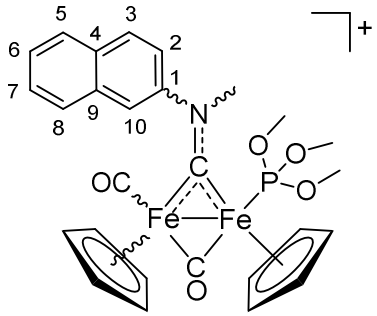

Chart S7. Structure of the cation within **3f** (wavy bonds refer to *cis*/*trans* isomerism).

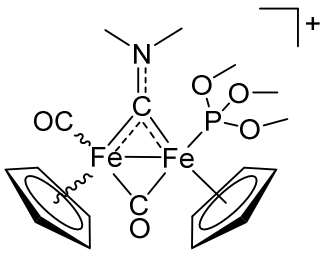

Chart S8. Structure of the cation within **4f**.

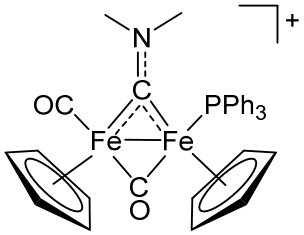

Chart S9. Structure of the cation within **5f** (wavy bonds refer to *cis*/*trans* isomerism)

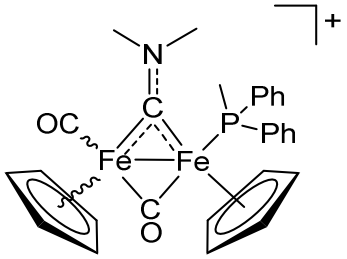

IR, NMR and ESI-MS spectra of diiron compounds

Figure S1. Solid-state IR spectrum (650-4000 cm^{-1}) of *cis-E*-[$Fe_2Cp_2(CO)(PTA)(\mu\text{-}CO)\{\mu\text{-}CNMe(Cy)\}]CF_3SO_3$, **2a**.

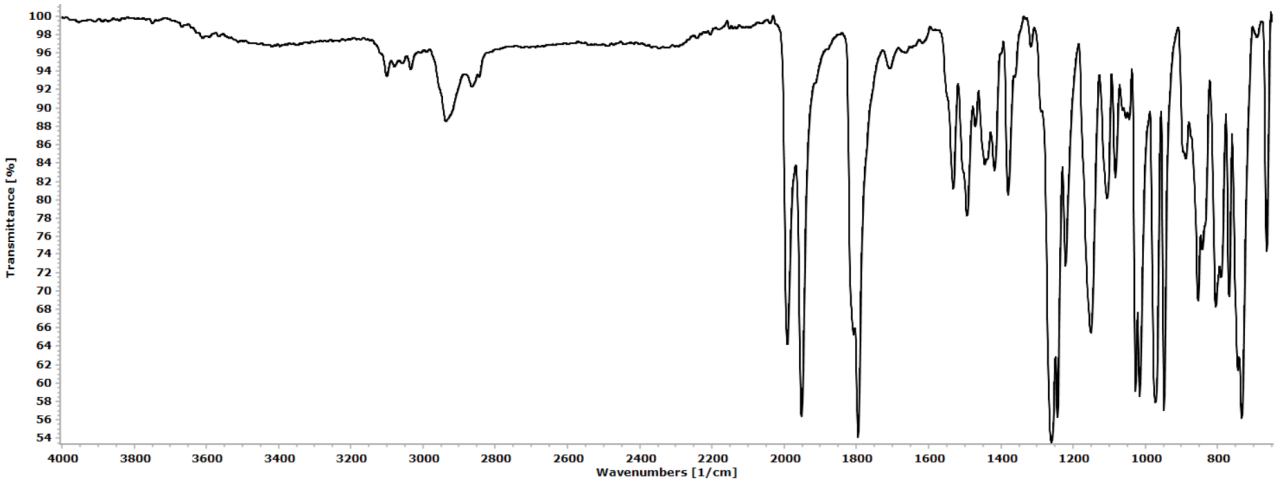

Figure S2. ^1H NMR spectrum (401 MHz, acetone-d_6) of *cis-E*-**2a**.

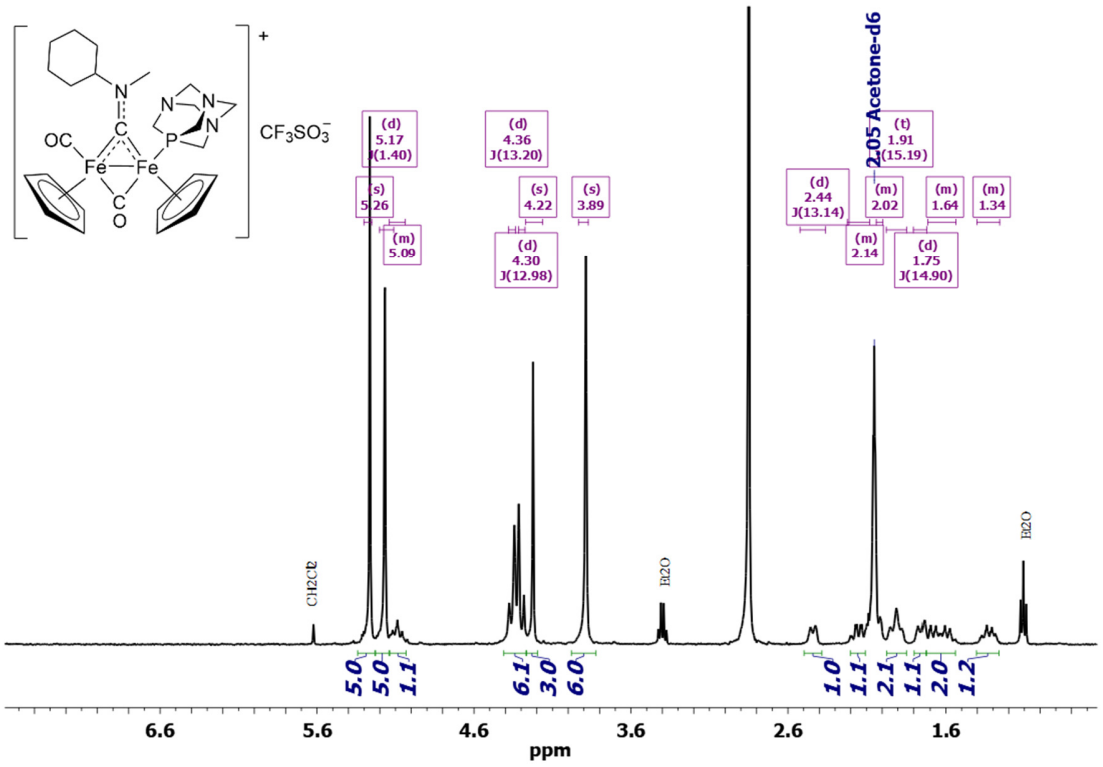

Figure S3. ^{1}H NMR spectrum (401 MHz, acetone-d_6) of **2a** (*cis*-*E*/*cis*-*Z* ratio = 5). Resonances due to *cis*-*Z*-**2a** are highlighted.

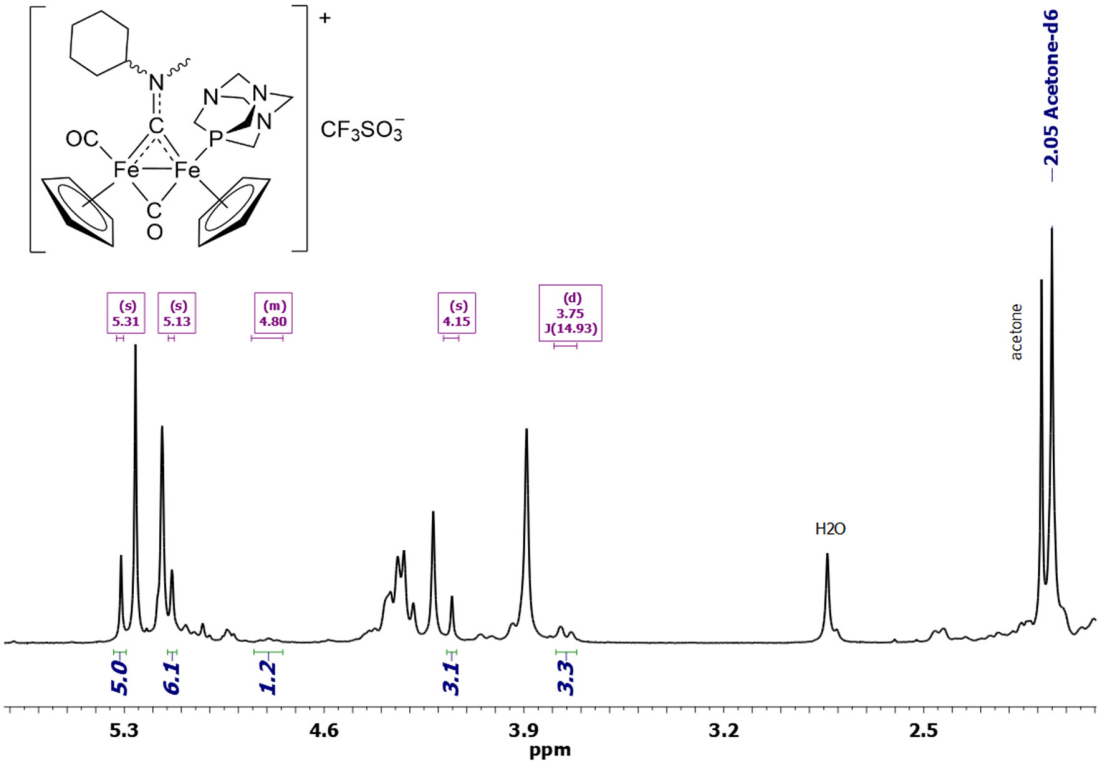

Figure S4. ^{13}C{^{1}H} NMR spectrum (101 MHz, acetone-d_6) of *cis*-*E*-**2a**.

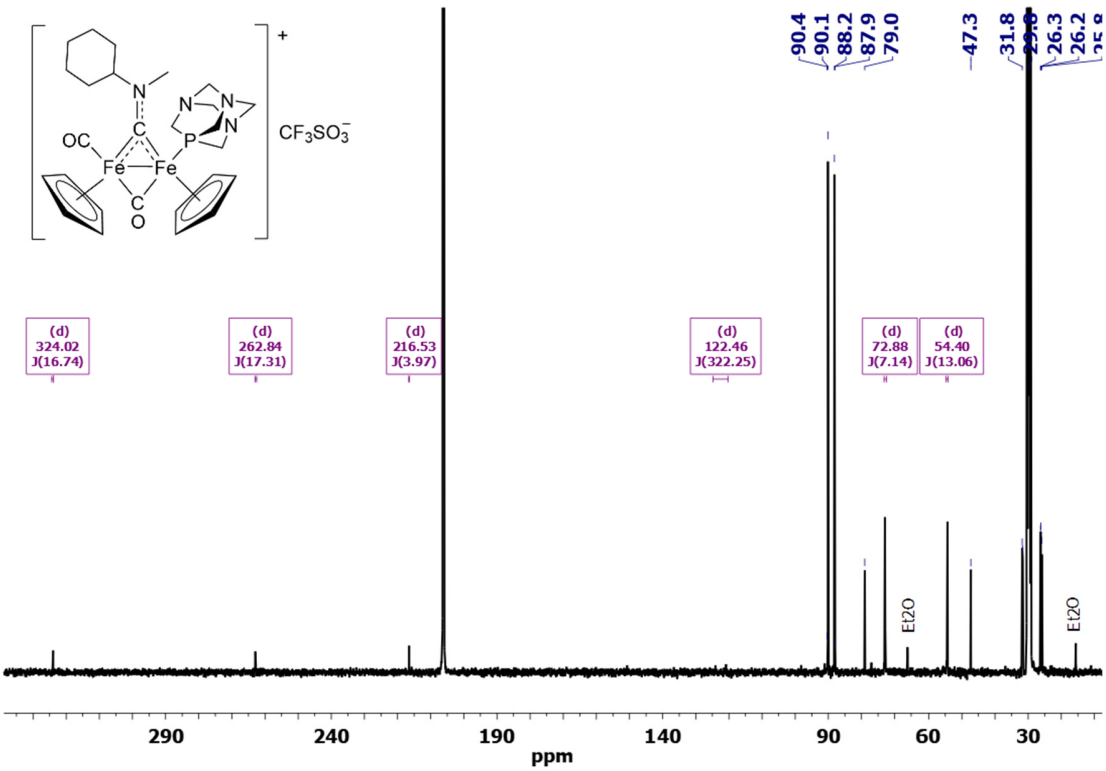

Figure S5. $^{31}P\{^{1}H\}$ NMR spectrum (162 MHz, acetone-d_6) of *cis-E*-**2a**.

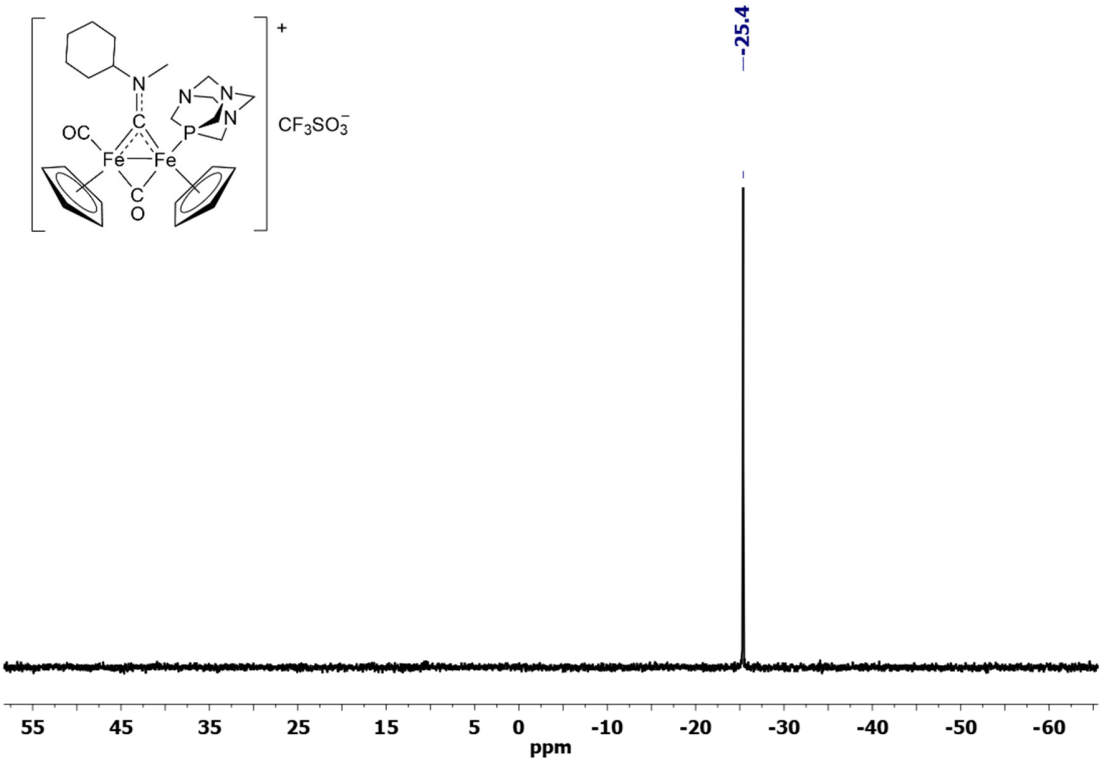

Figure S6. $^{31}P\{^{1}H\}$ NMR spectrum (162 MHz, acetone-d_6) of **2a** (*cis-E*/*cis-Z* ratio = 5).

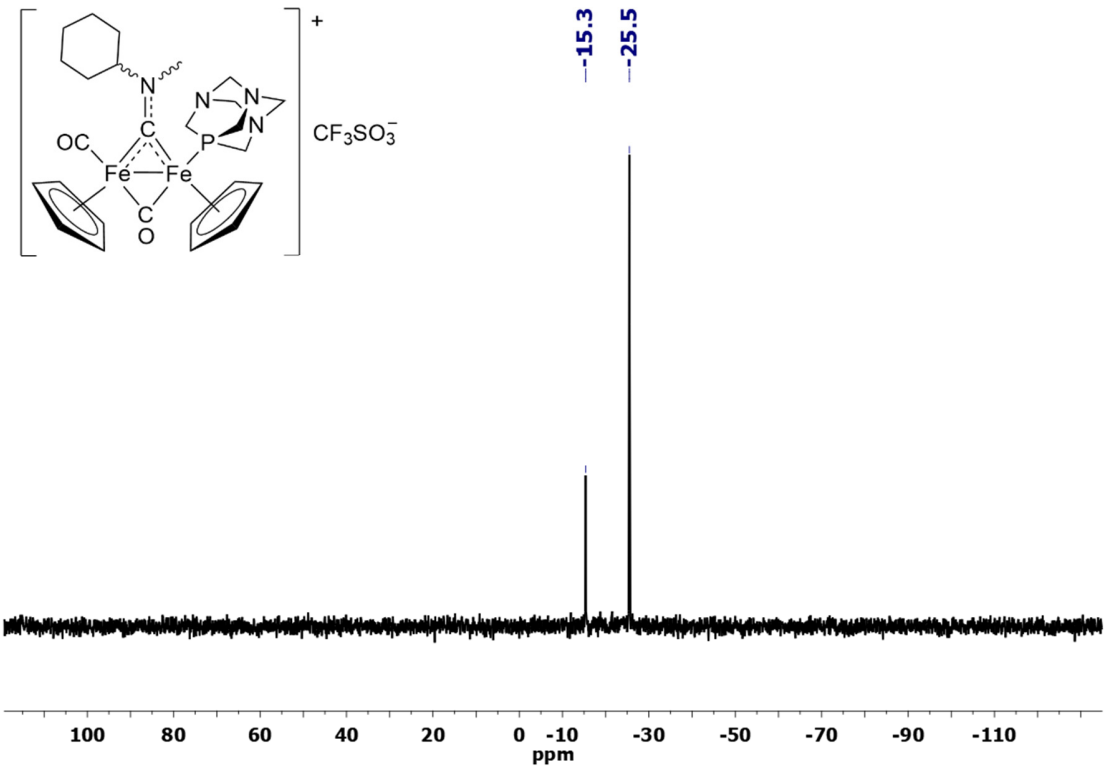

Figure S7. Black line: ^{1}H NMR spectrum (401 MHz, acetone-d_6) of *cis-E*-**2a**. Blue line: ^{1}H NOESY with irradiation at 5.17 ppm (Cp^P). Red line: ^{1}H NOESY with irradiation at 5.26 ppm (Cp). Observed NOEs are indicated by the arrows.

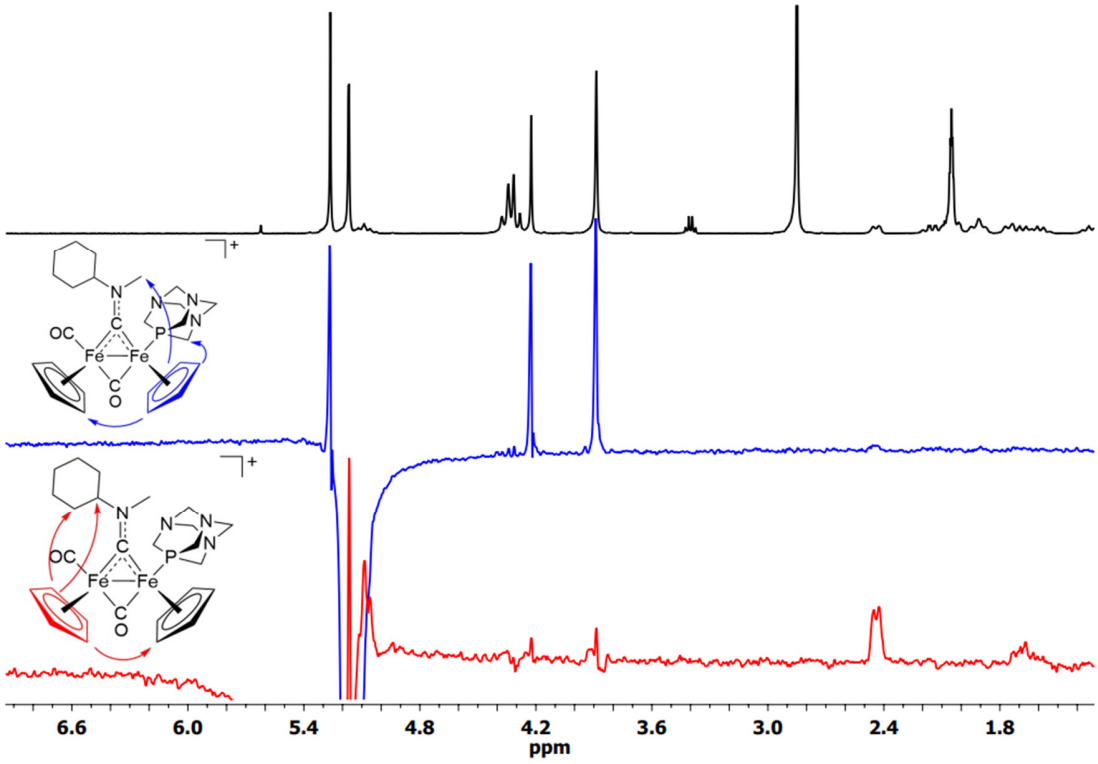

Figure S8. Solid-state IR spectrum (650-4000 cm^{-1}) of $[Fe_2Cp_2(CO)(PTA)(\mu\text{-}CO)\{\mu\text{-}CNMe(4\text{-}C_6H_4OMe)\}]CF_3SO_3$, **2b** (*cis-E*/*cis-Z* ratio: 20).

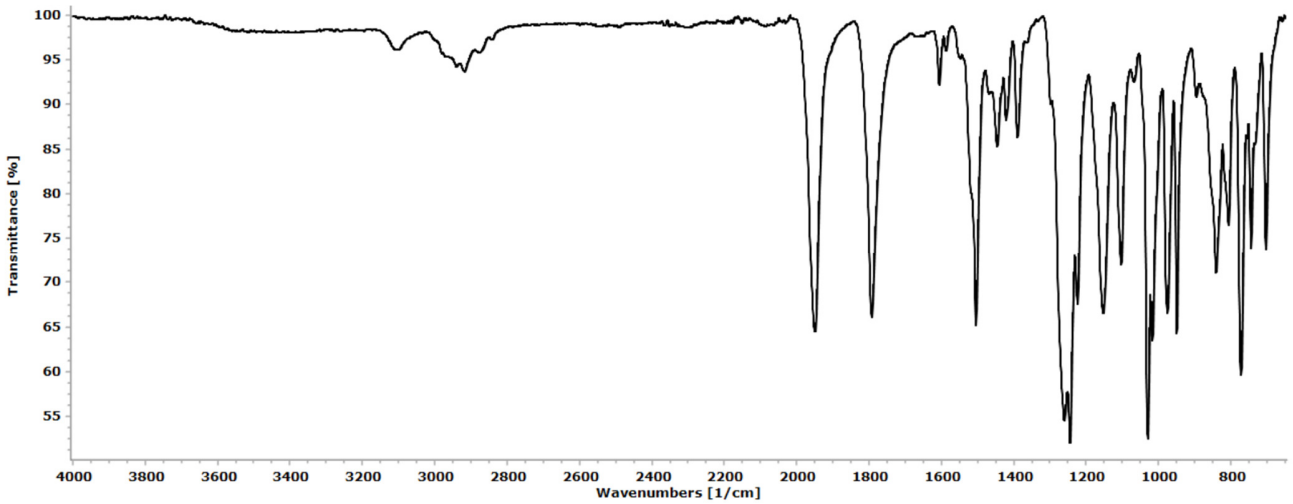

Figure S9. ^{1}H NMR spectrum (401 MHz, acetone-d_6) of **2b** (*cis-E*/*cis-Z* ratio = 20).

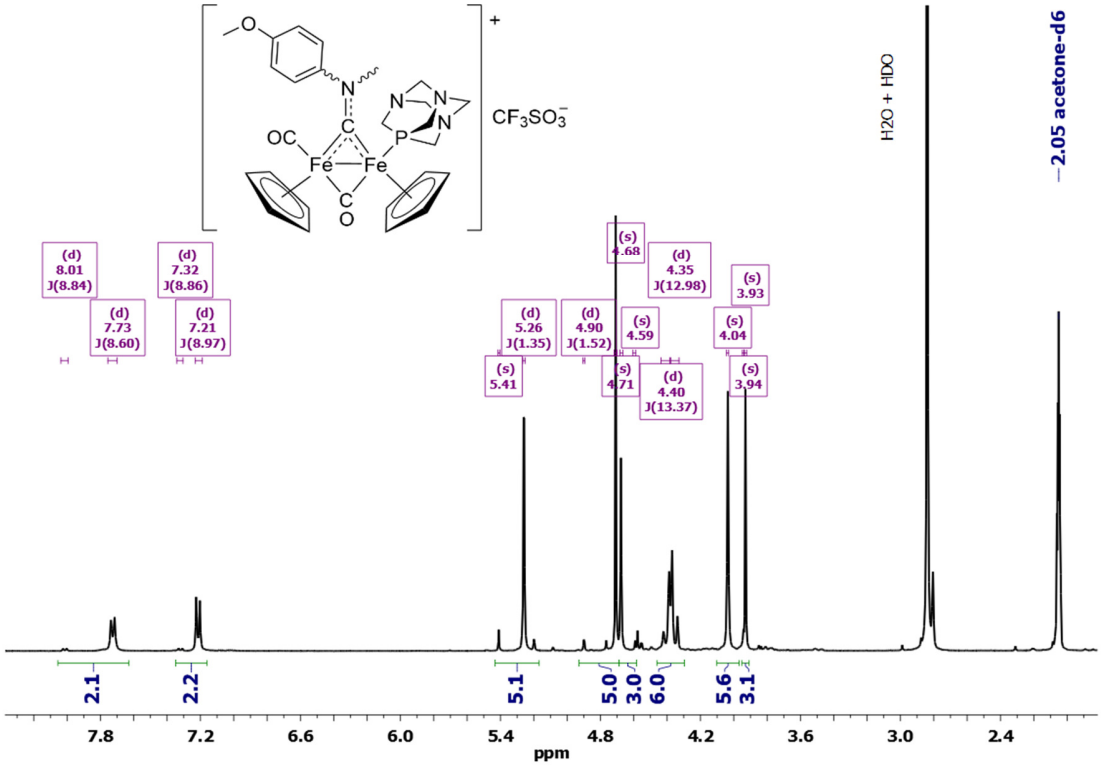

Figure S10. $^{13}C\{^{1}H\}$ NMR spectrum (101 MHz, acetone-d_6) of **2b** (*cis-E*/*cis-Z* ratio = 20).

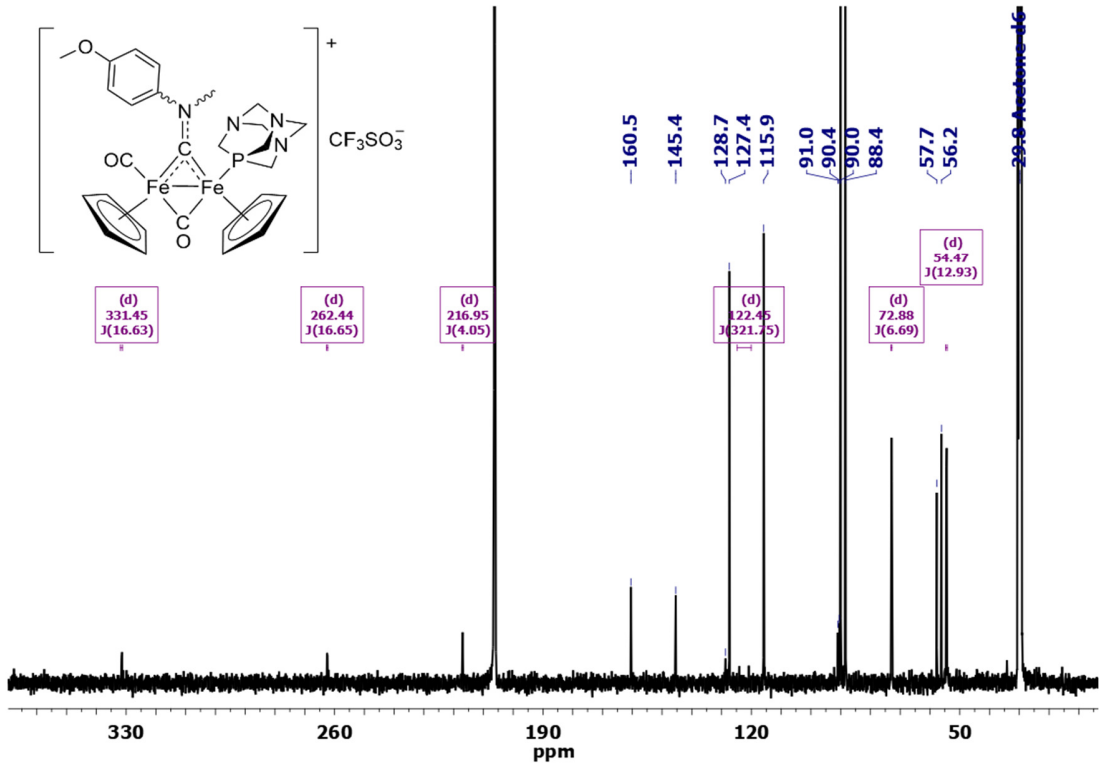

Figure S11. $^{31}P\{^{1}H\}$ NMR spectrum (162 MHz, acetone-d_6) of **2b** (*cis-E*/*cis-Z* ratio = 20).

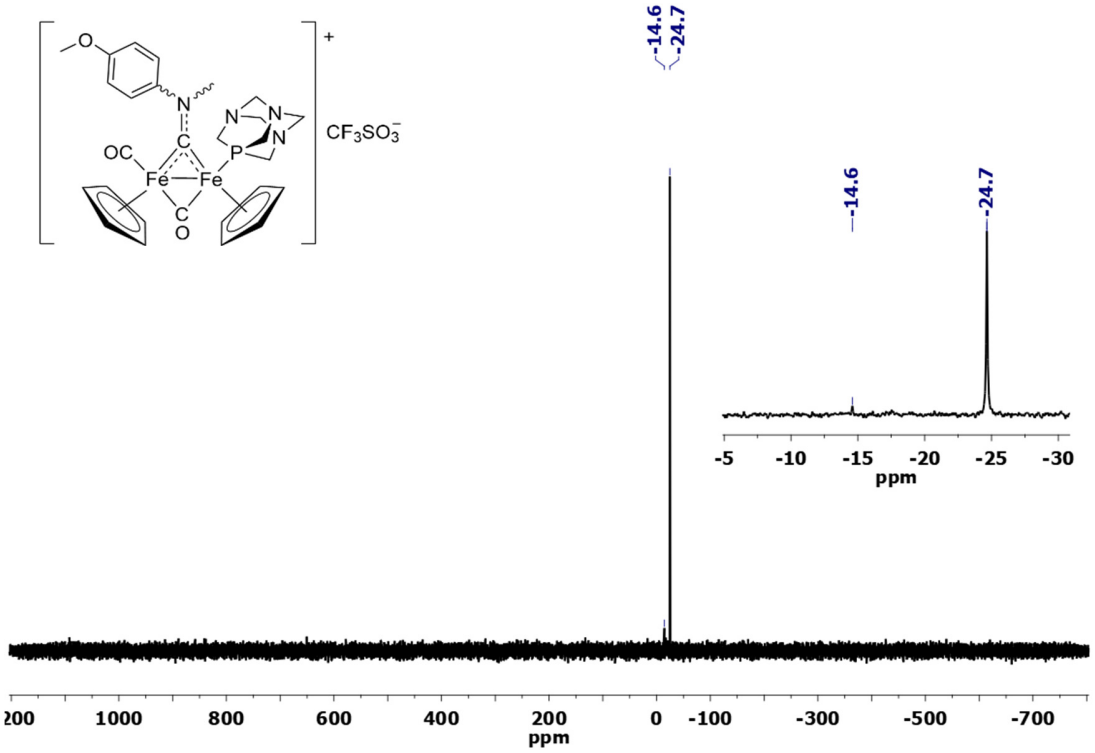

Figure S12. Black line: ^{1}H NMR spectrum (401 MHz, acetone-d_6) of *cis-E*-**2b**. Blue line: ^{1}H NOESY with irradiation at 5.26 ppm (Cp^{P}). Red line: ^{1}H NOESY with irradiation at 4.70 ppm (Cp). Observed NOEs are indicated by the arrows.

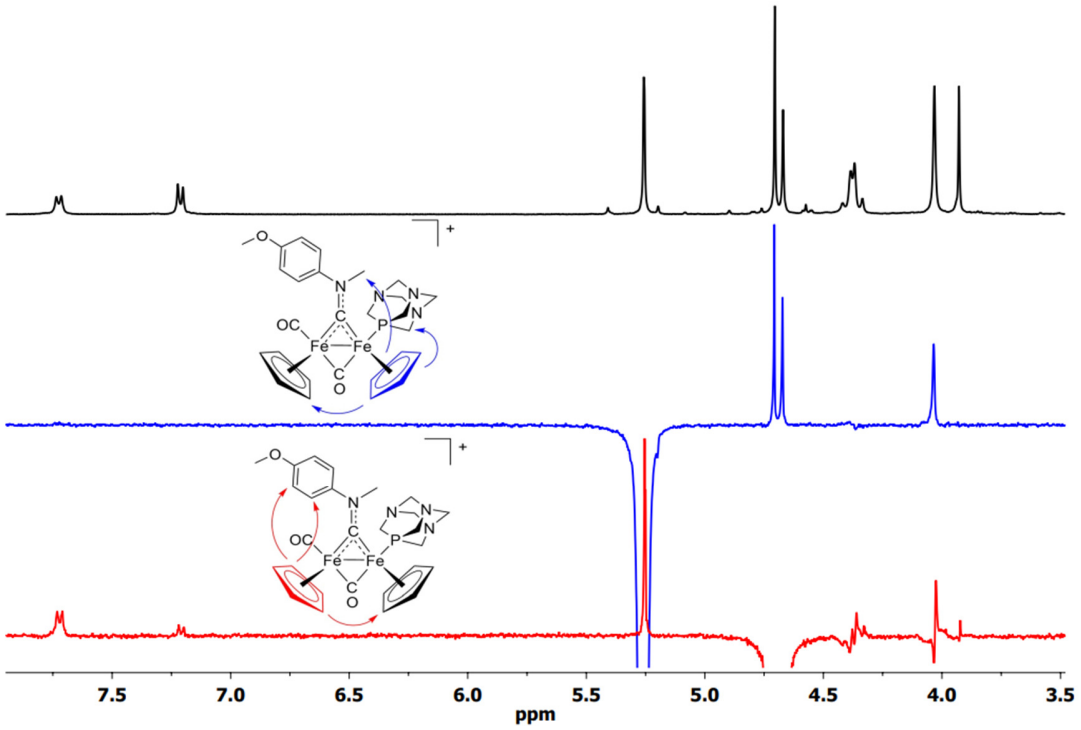

Figure S13. Solid-state IR spectrum (650-4000 cm^{-1}) of $[Fe_2Cp_2(CO)(PTA)(\mu\text{-}CO)\{\mu\text{-}CNMe(2\text{-}naphthyl)\}]CF_3SO_3$, **2c** (*cis-E*/*cis-Z* ratio = 7).

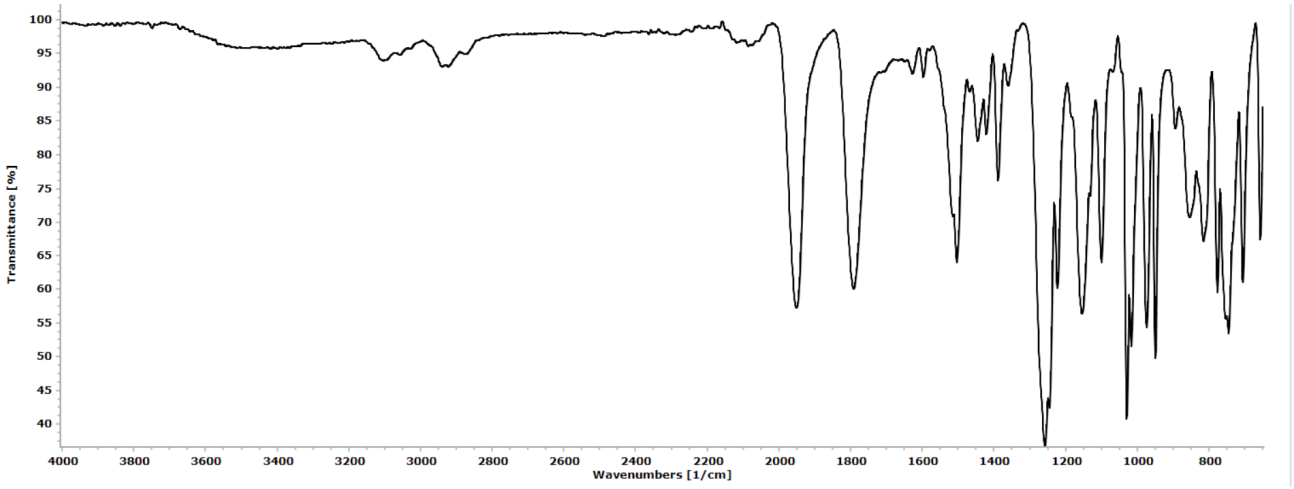

Figure S14. ^1H NMR spectrum (401 MHz, acetone-d_6) of **2c** (*cis-E*/*cis-Z* ratio = 7).

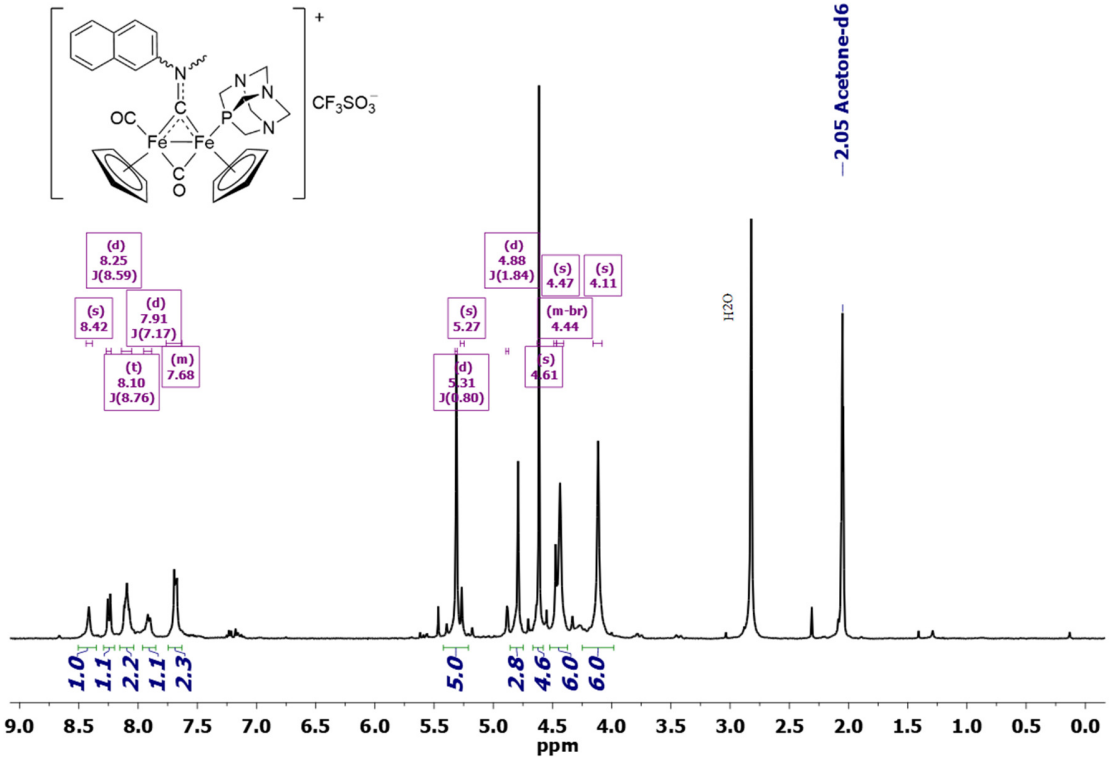

Figure S15. $^{13}C\{^{1}H\}$ NMR spectrum (101 MHz, acetone-d_6) of **2c** (*cis-E*/*cis-Z* ratio = 7).

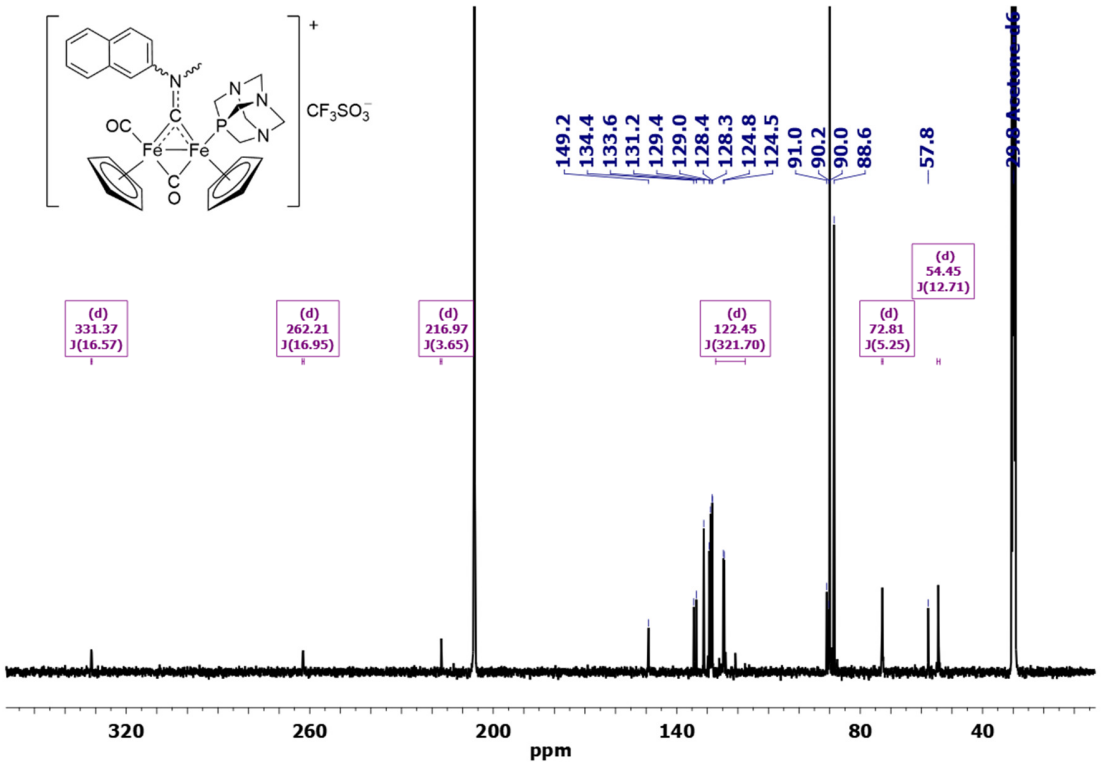

Figure S16. $^{31}P\{^{1}H\}$ NMR spectrum (162 MHz, acetone-d_6) of **2c** (*cis-E*/*cis-Z* ratio = 7).

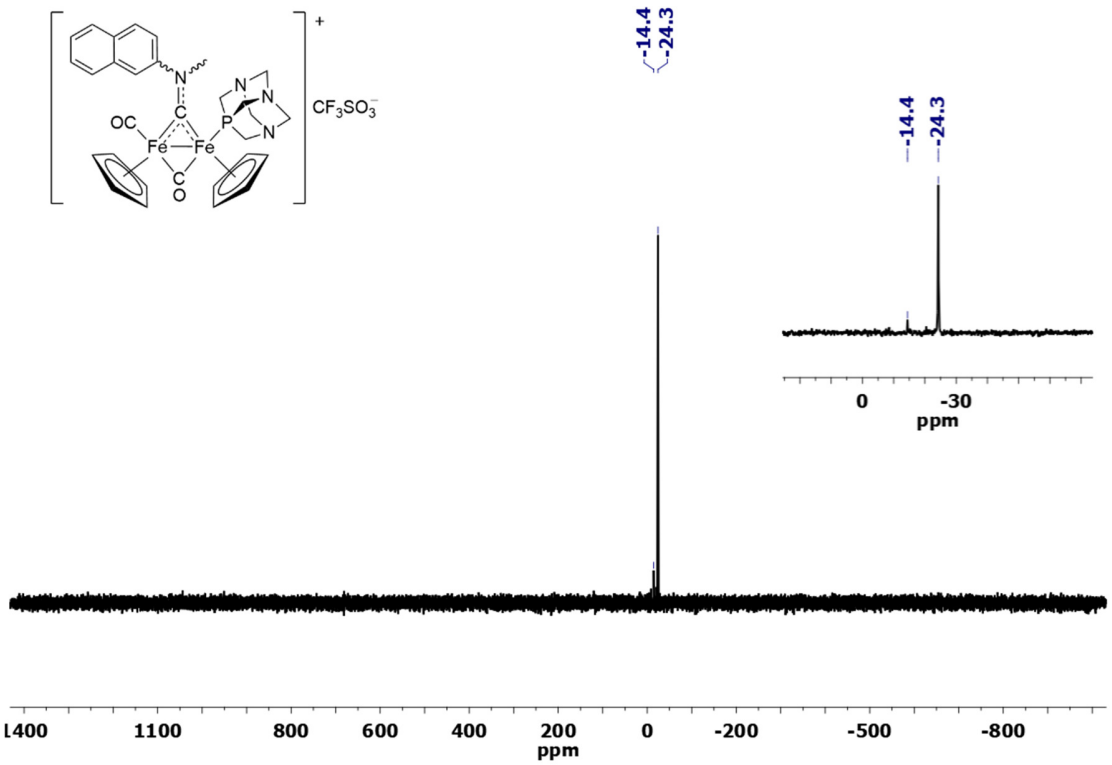

Figure S17. Black line: ^{1}H NMR spectrum (401 MHz, acetone-d_6) of *cis-E*-**2c**. Blue line: ^{1}H NOESY with irradiation at 5.31 ppm (Cp^{P}). Red line: ^{1}H NOESY with irradiation at 4.61 ppm (Cp). Observed NOEs are indicated by the arrows.

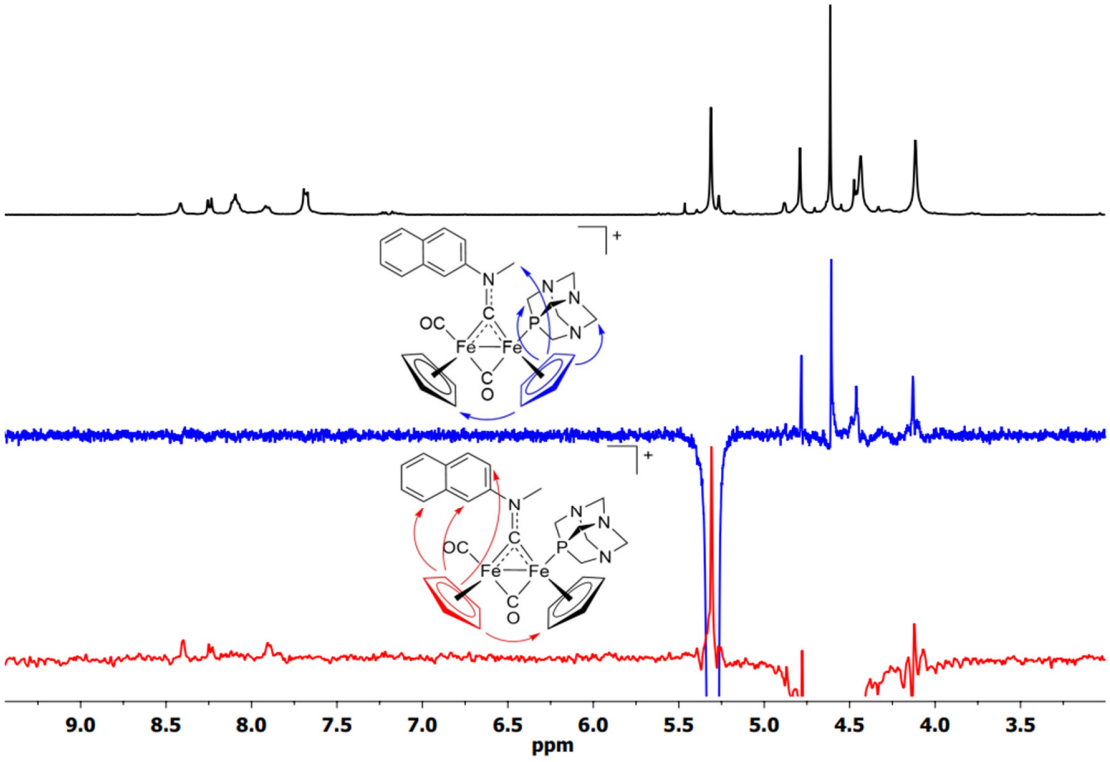

Figure S18. Solid-state IR spectrum (650-4000 cm^{-1}) of $[Fe_2Cp_2(CO)(PTA)(\mu\text{-}CO)(\mu\text{-}CNBn_2)]CF_3SO_3$, **2d** (*cis*/*trans* ratio = 15).

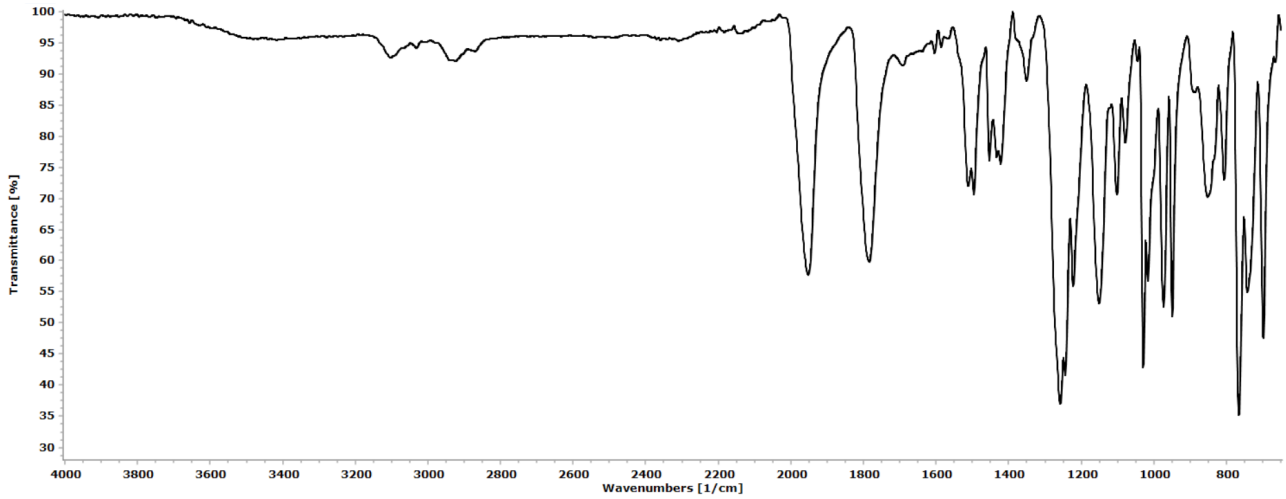

Figure S19. ^{1}H NMR spectrum (401 MHz, acetone-d_6) of **2d** (*cis*/*trans* ratio = 15). The resonance at 3.80 is due to an impurity in acetone-d_6. Only resonances due to the *cis* isomers are integrated.

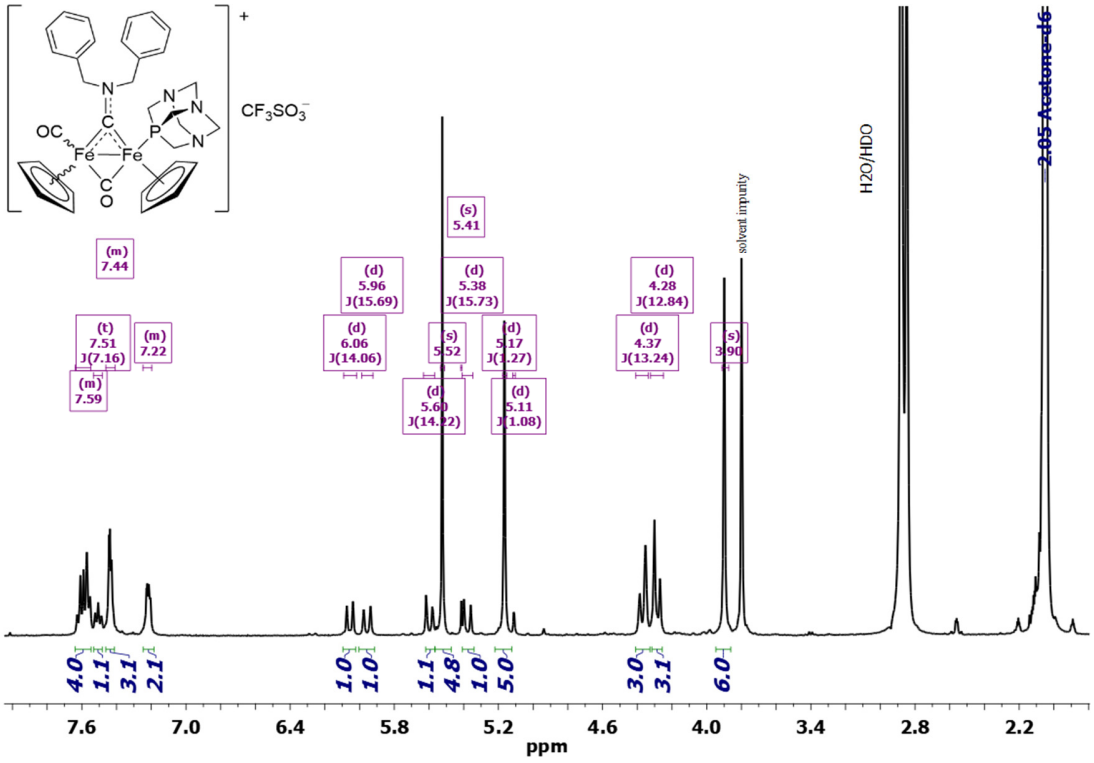

Figure S20. ^{13}C{^{1}H} NMR spectrum (101 MHz, acetone-d_6) of **2d** (*cis*/*trans* ratio = 15).

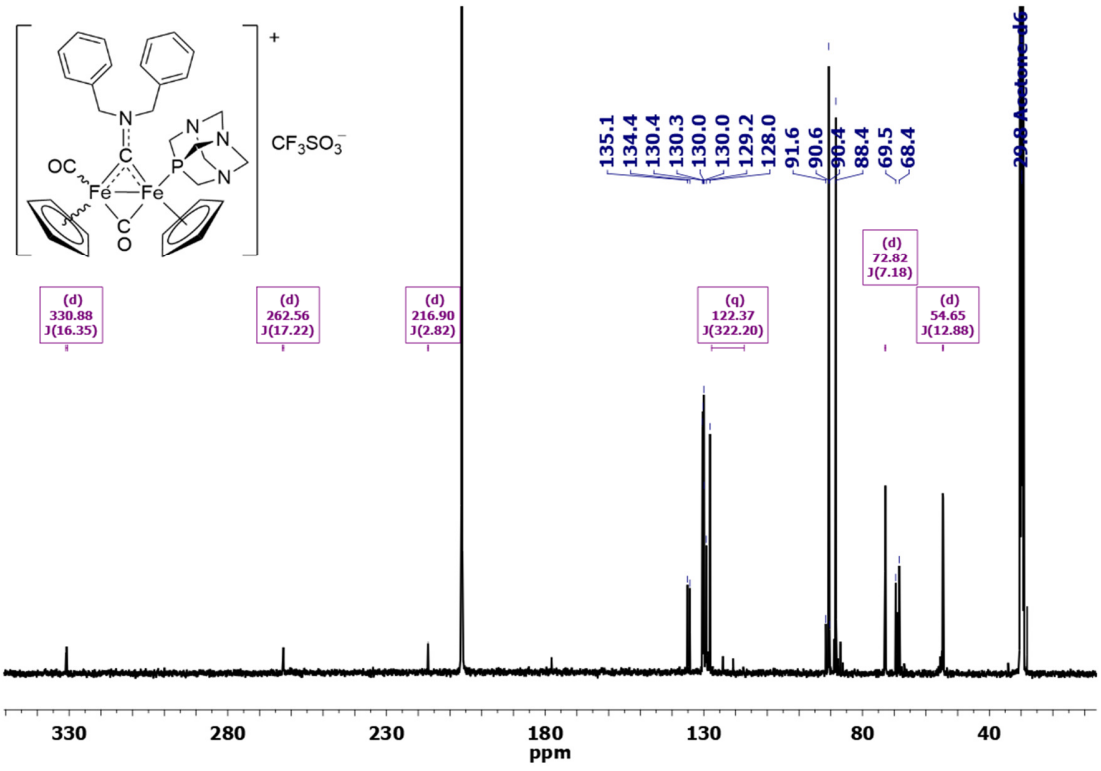

Figure S21. $^{31}P\{^{1}H\}$ NMR spectrum (162 MHz, acetone-d_6) of **2d** (*cis*/*trans* ratio = 15).

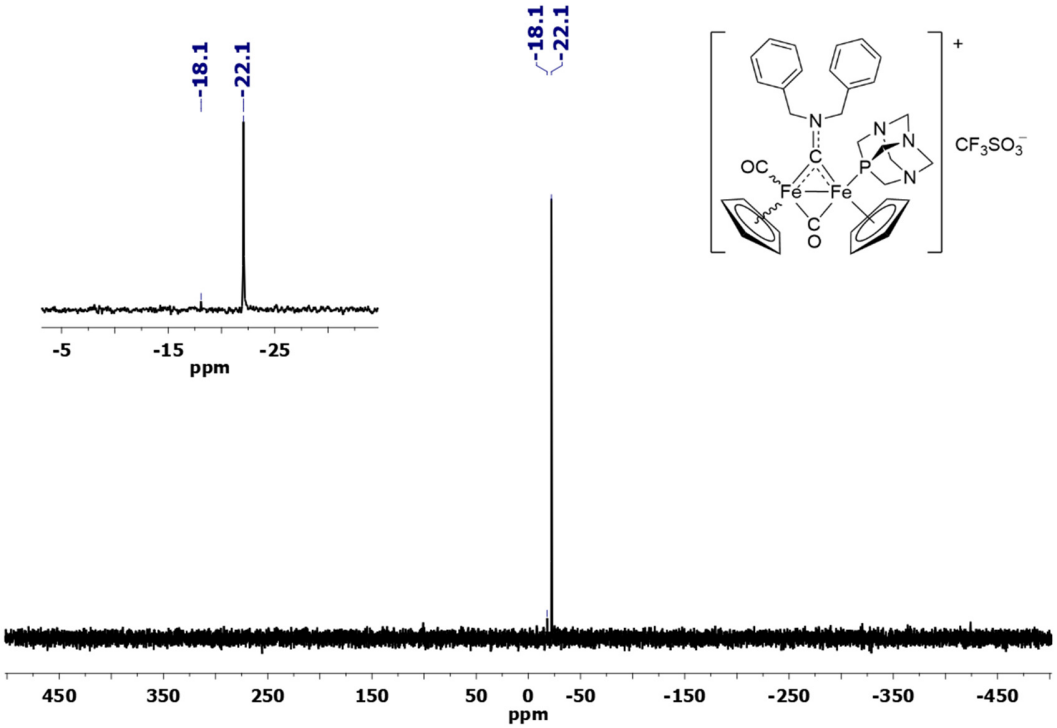

Figure S22. Black line: ^{1}H NMR spectrum (401 MHz, acetone-d_6) of *cis*-**2d**. Blue line: ^{1}H NOESY with irradiation at 5.17 ppm (Cp^P). Red line: ^{1}H NOESY with irradiation at 5.53 ppm (Cp). Observed NOEs are indicated by the arrows.

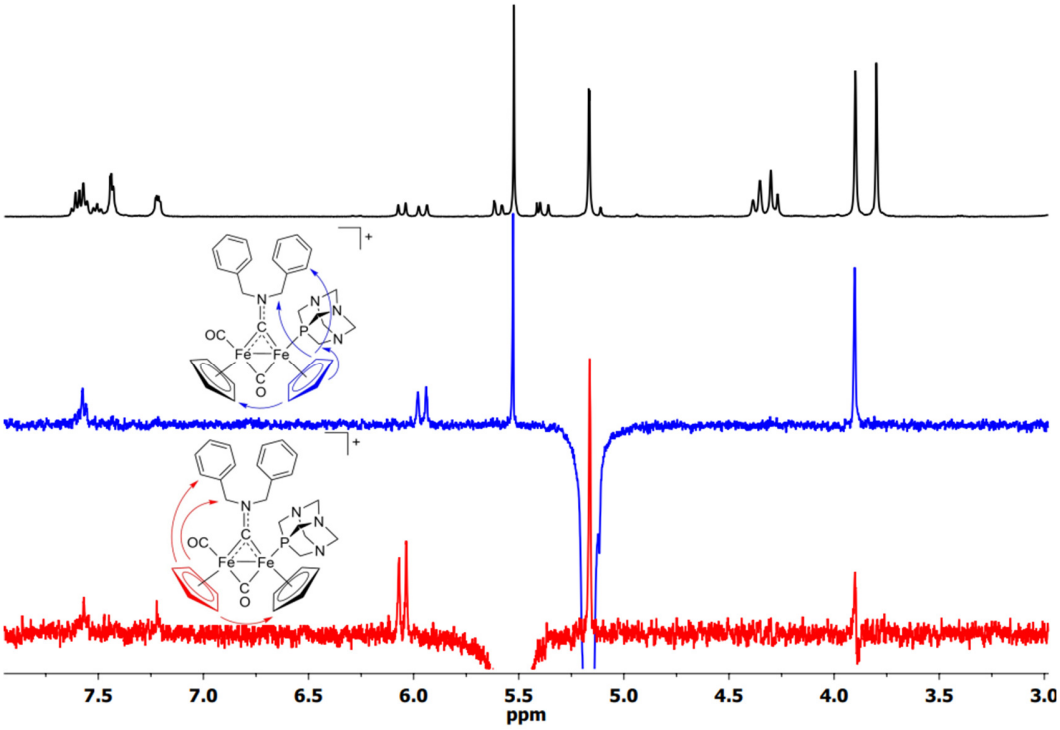

Figure S23. Solid-state IR spectra (650-4000 cm^{-1}) of two samples of $[Fe_2Cp_2(CO)(PTA)(\mu\text{-}CO)\{\mu\text{-}CNMe(Xyl)\}]CF_3SO_3$, **2e** with *cis-E*/*cis-Z* ratio 0.2 (1:4; blue line) or 1.1 (red line).

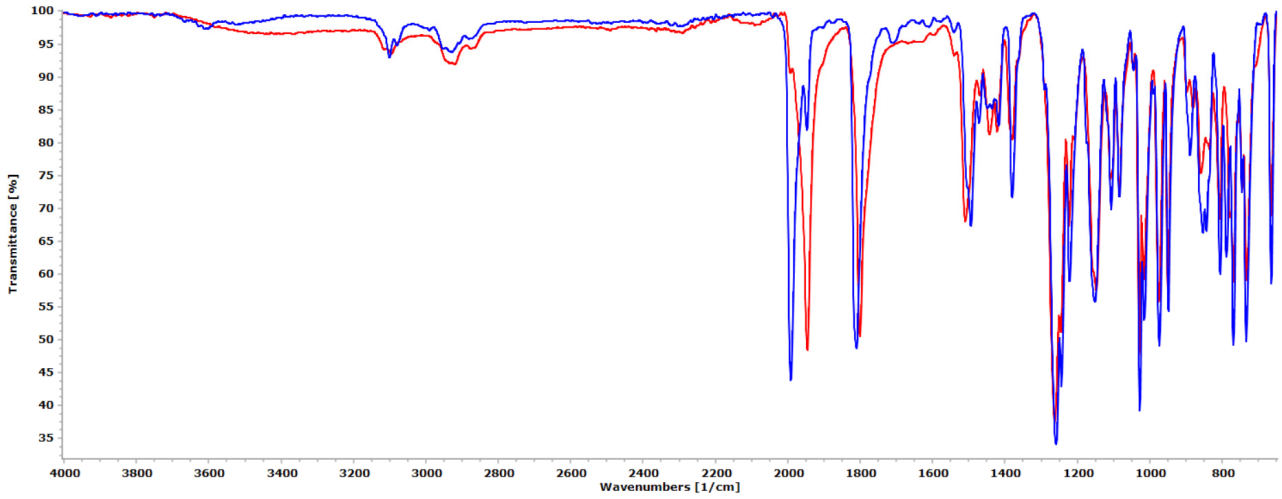

Figure S24. ^1H NMR spectrum (401 MHz, DMSO-d_6) of **2e** (*cis-E*/*cis-Z* ratio = 1.1).

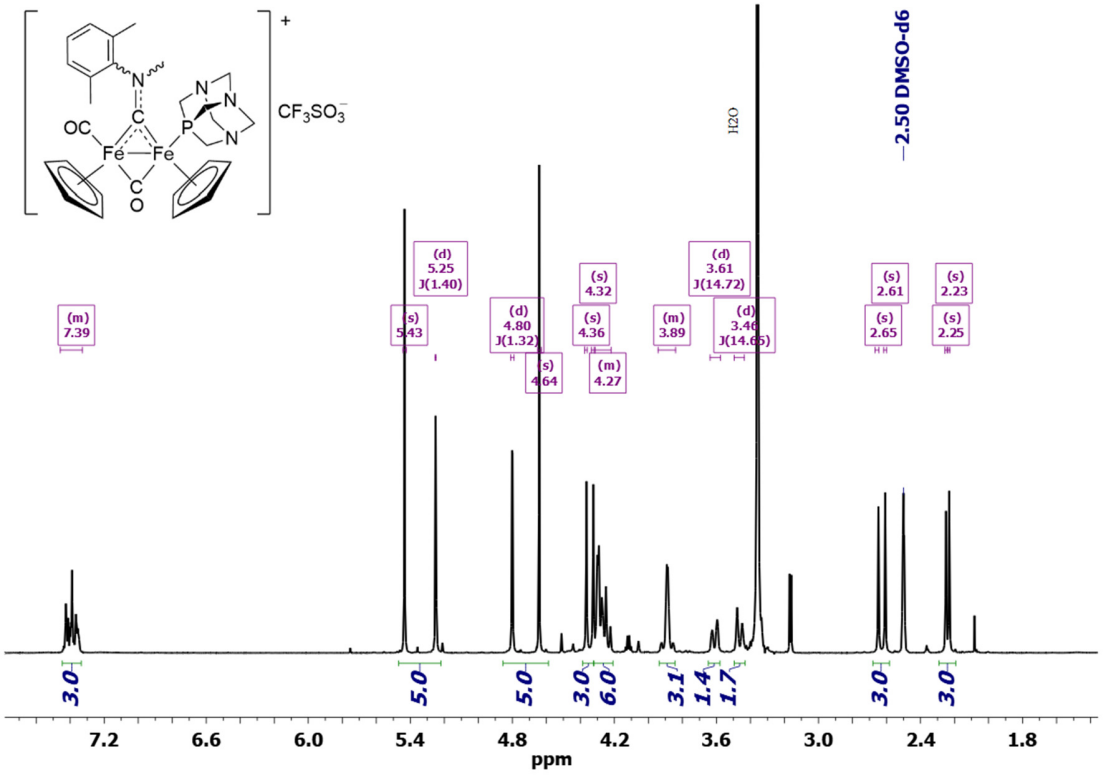

Figure S25. $^{13}C\{^{1}H\}$ NMR spectrum (101 MHz, DMSO-d_6) of **2e** (*cis-E*/*cis-Z* ratio = 1.1).

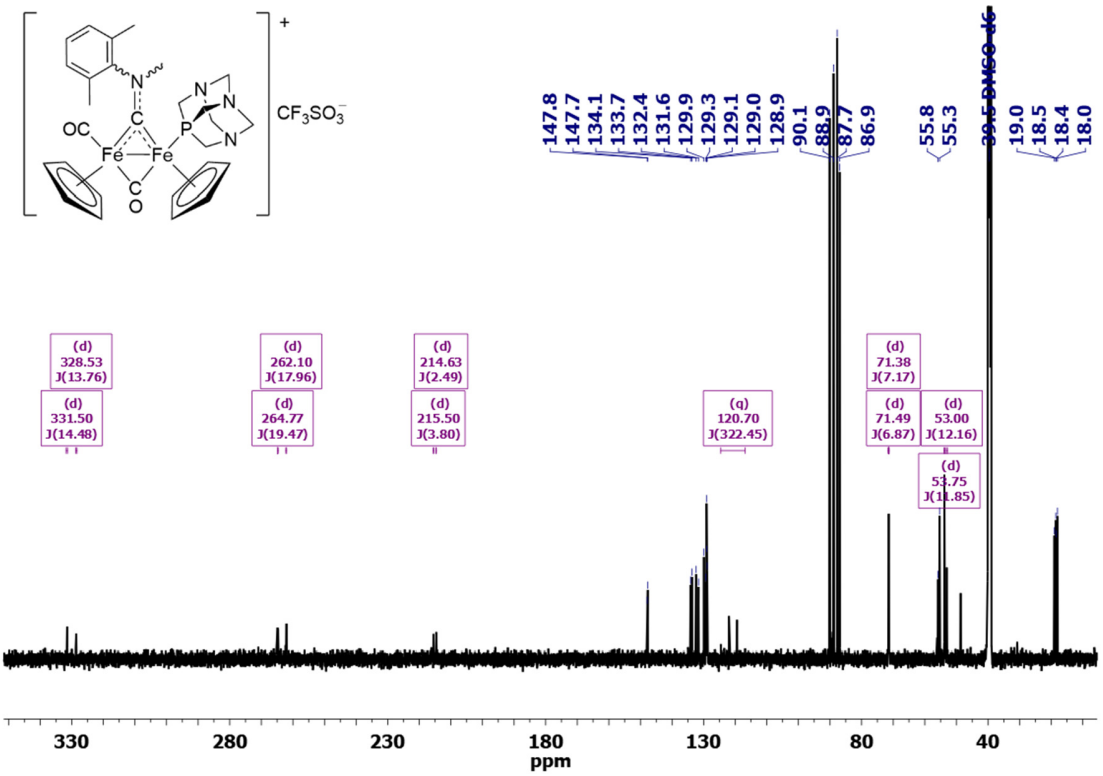

Figure S26. $^{31}P\{^{1}H\}$ NMR spectrum (162 MHz, DMSO-d_6) of **2e** (*cis-E*/*cis-Z* ratio = 1.1).

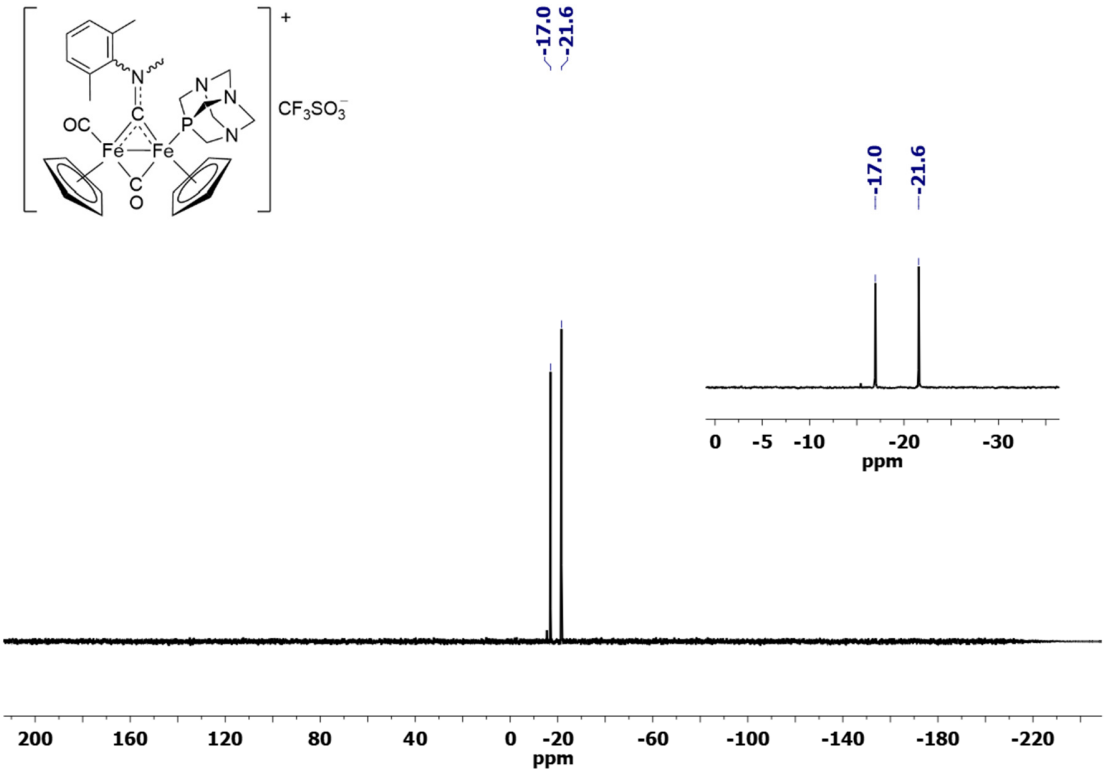

Figure S27. Solid-state IR spectrum (650-4000 cm^{-1}) of $[Fe_2Cp_2(CO)\{P(OMe)_3\}(\mu\text{-}CO)\{\mu\text{-}CNMe(2\text{-naphthyl})\}]CF_3SO_3$, **3c** (*cis*-*E*/*trans*-*E*/*cis*-*Z* ratio = 13:1.6:1).

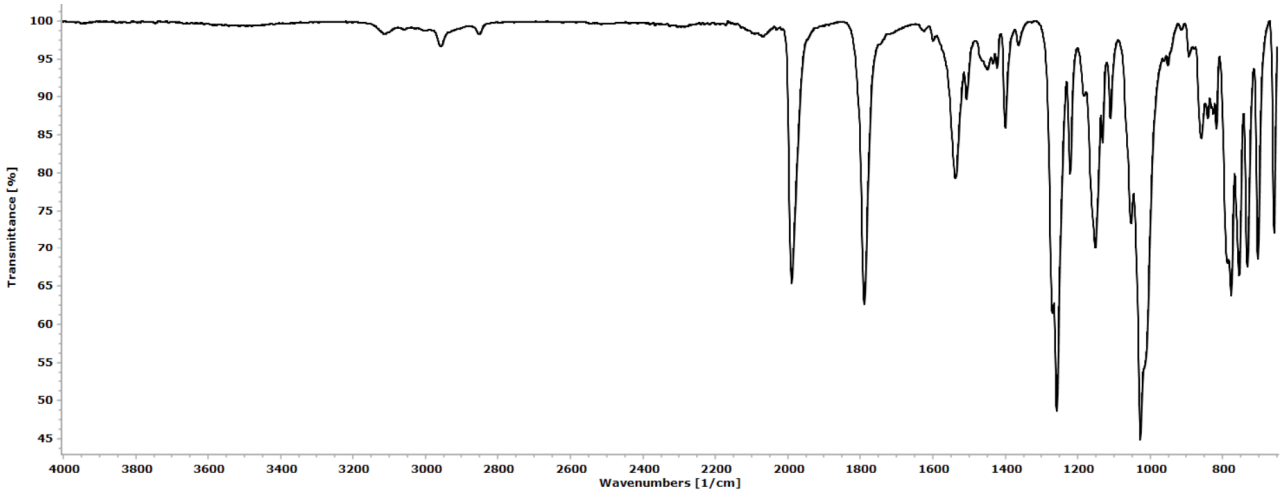

Figure S28. ^1H NMR spectrum (401 MHz, acetone-d_6) of **3c** (*cis*-*E*/*trans*-*E*/*cis*-*Z* ratio = 13:1.6:1).

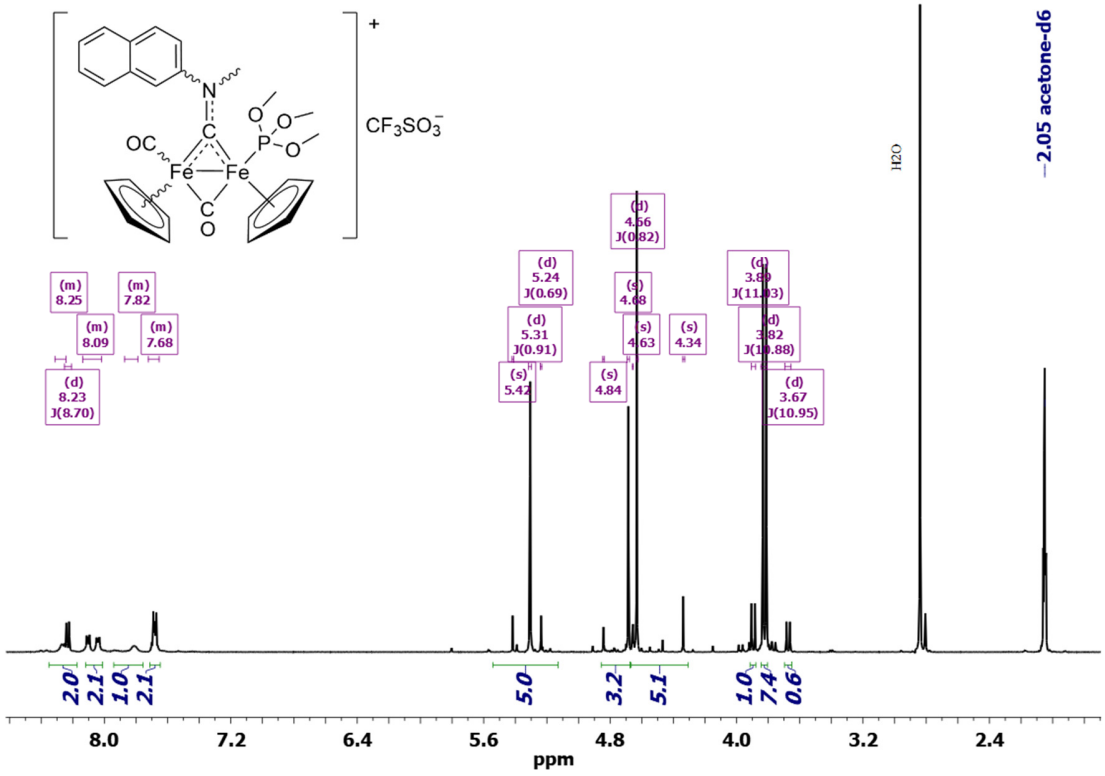

Figure S29. $^{13}C\{^{1}H\}$ NMR spectrum (101 MHz, acetone-d_6) of **3c** (*cis-E*/*trans-E*/*cis-Z* ratio = 13:1.6:1).

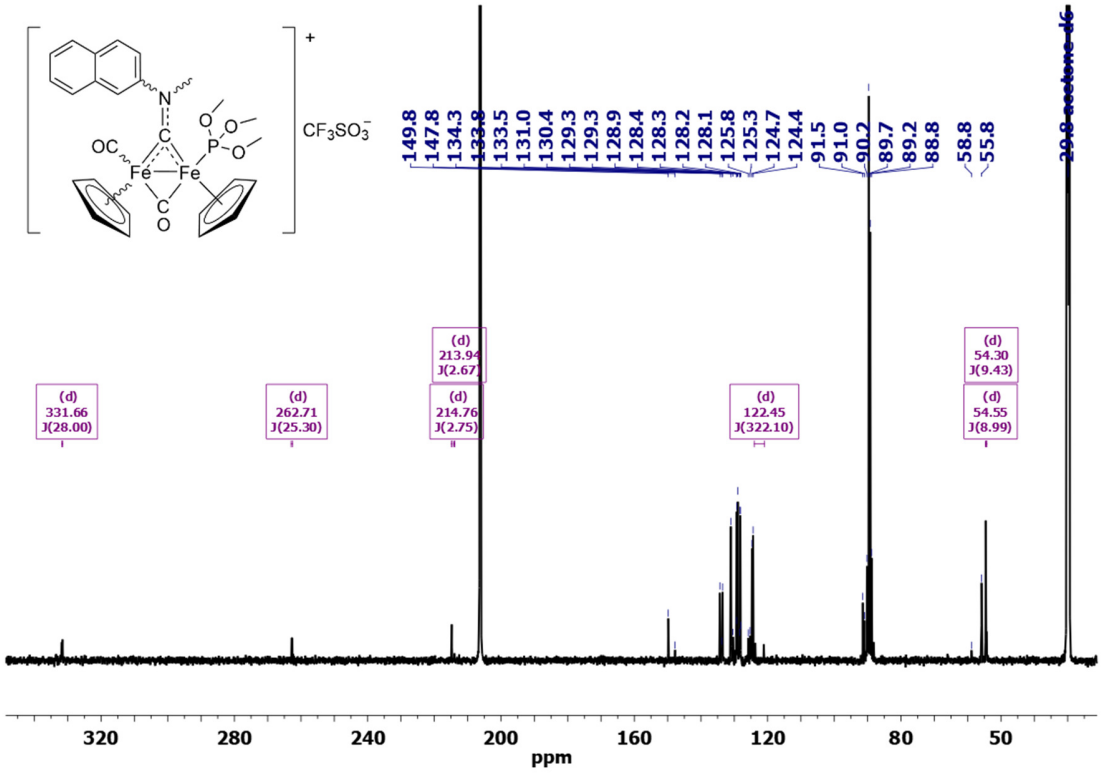

Figure S30. $^{31}P\{^{1}H\}$ NMR spectrum (162 MHz, acetone-d_6) of **3c** (*cis-E*/*trans-E*/*cis-Z* ratio = 13:1.6:1).

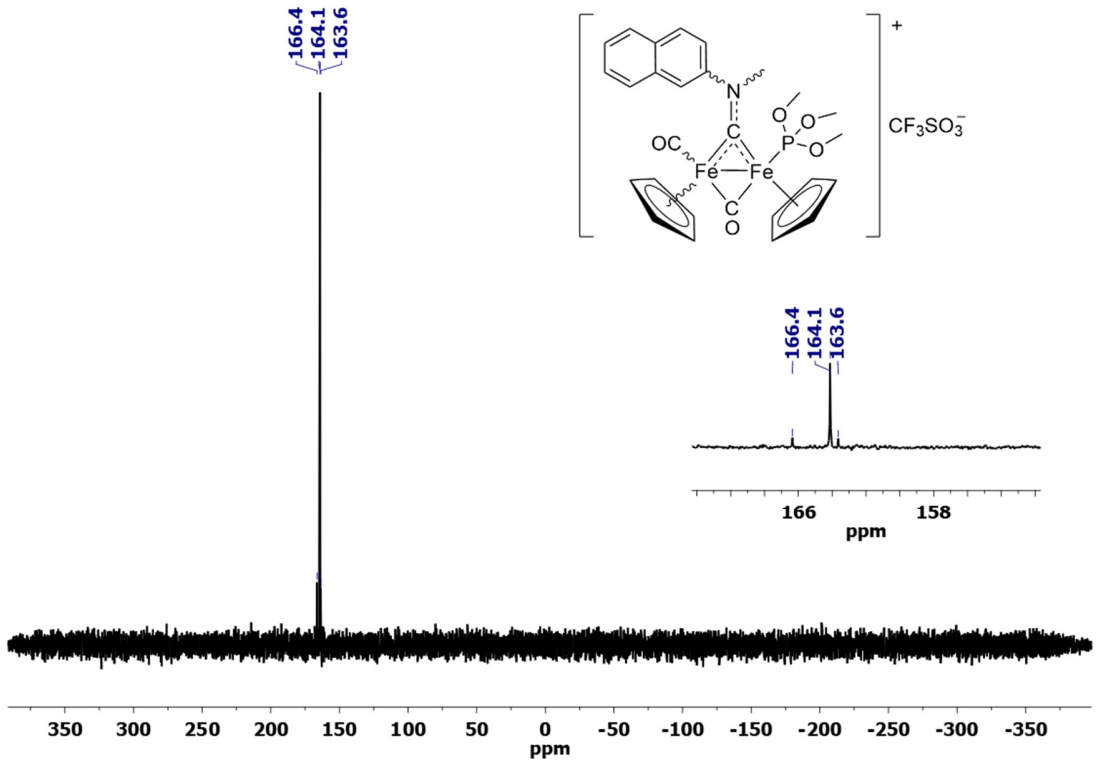

Figure S31. Black line: ^{1}H NMR spectrum (401 MHz, acetone-d_6) of **3c**. Blue line: ^{1}H NOESY with irradiation at 5.31 ppm (Cp^P of the *cis-E* isomer). Red line: ^{1}H NOESY with irradiation at 5.24 ppm (Cp^P of the *trans-E* isomer). Observed NOEs are indicated by the arrows.

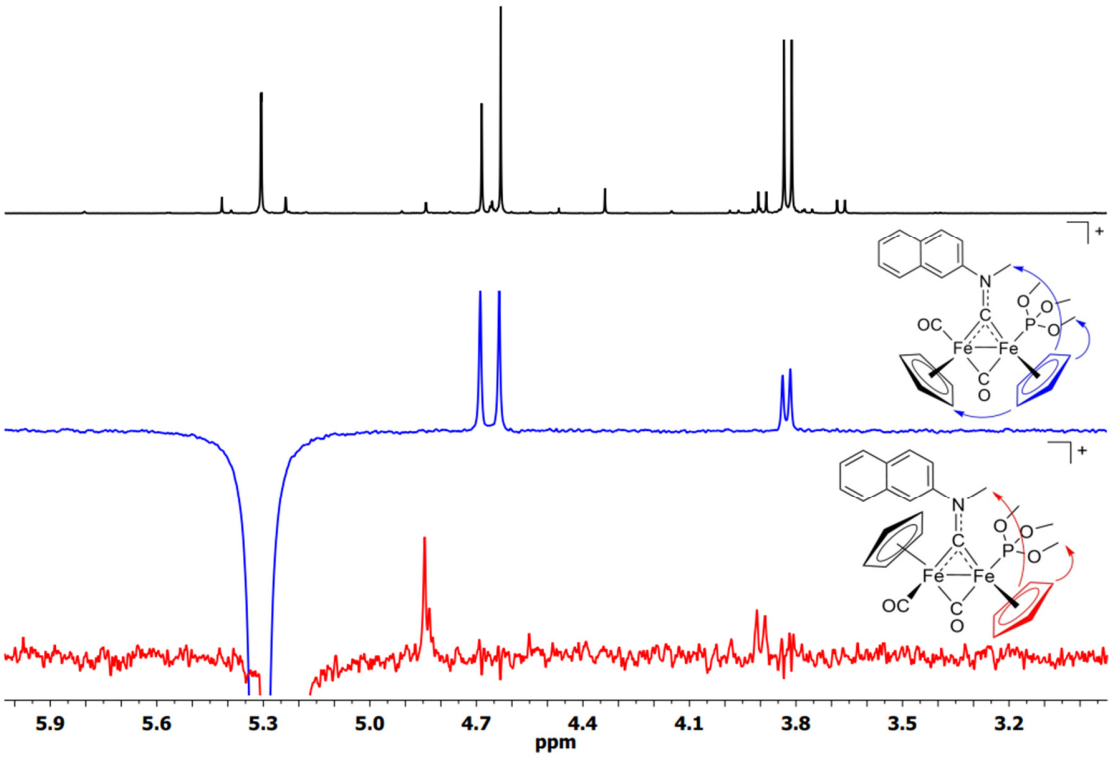

Figure S32. Solid-state IR spectrum (650-4000 cm^{-1}) of $[Fe_2Cp_2(CO)\{P(OMe)_3\}(\mu\text{-}CO)(\mu\text{-}CNMe_2)]CF_3SO_3$, **3f** (*cis*/*trans* ratio ≈ 18).

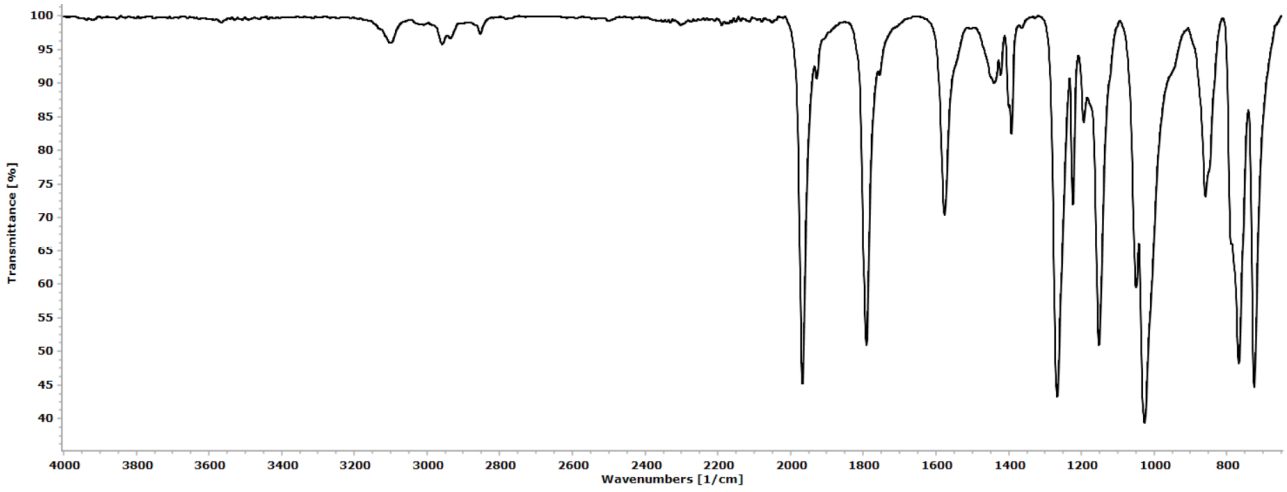

Figure S33. ^{1}H NMR spectrum (401 MHz, acetone-d_6) of **3f** (*cis*/*trans* ratio ≈ 18). Integrals refer to the resonances of the *cis* isomer only.

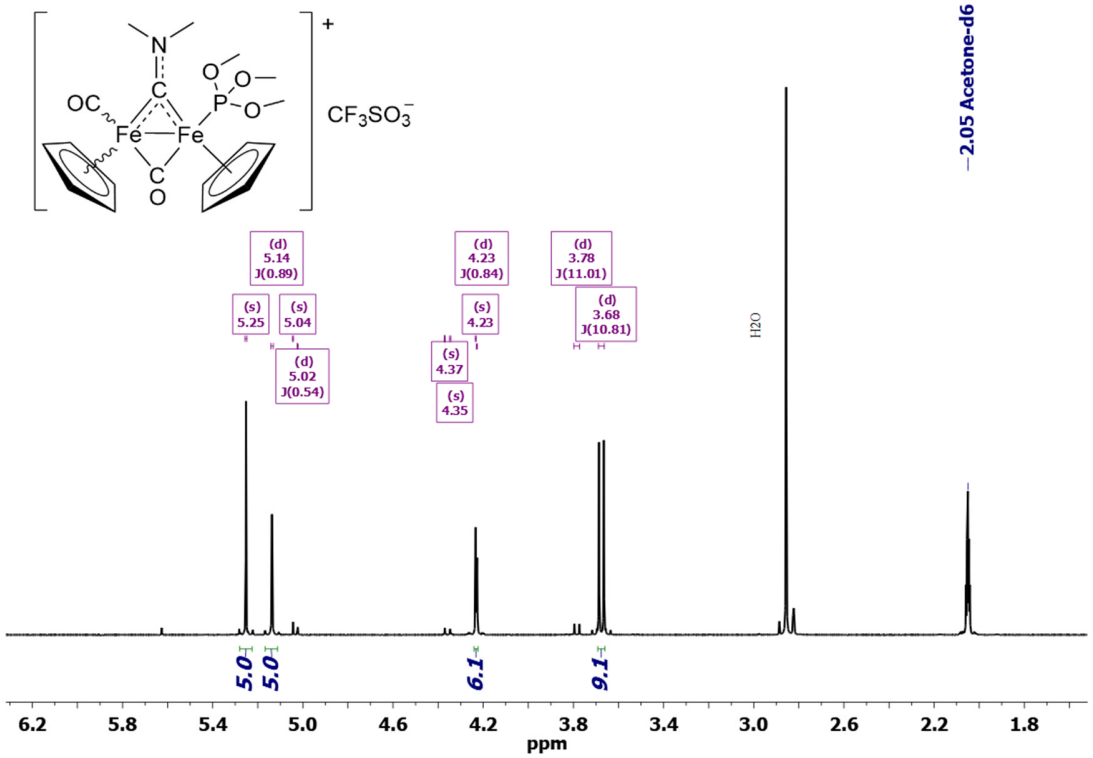

Figure S34. ^{13}C{^{1}H} NMR spectrum (101 MHz, acetone-d_6) of **3f** (*cis*/*trans* ratio ≈ 18).

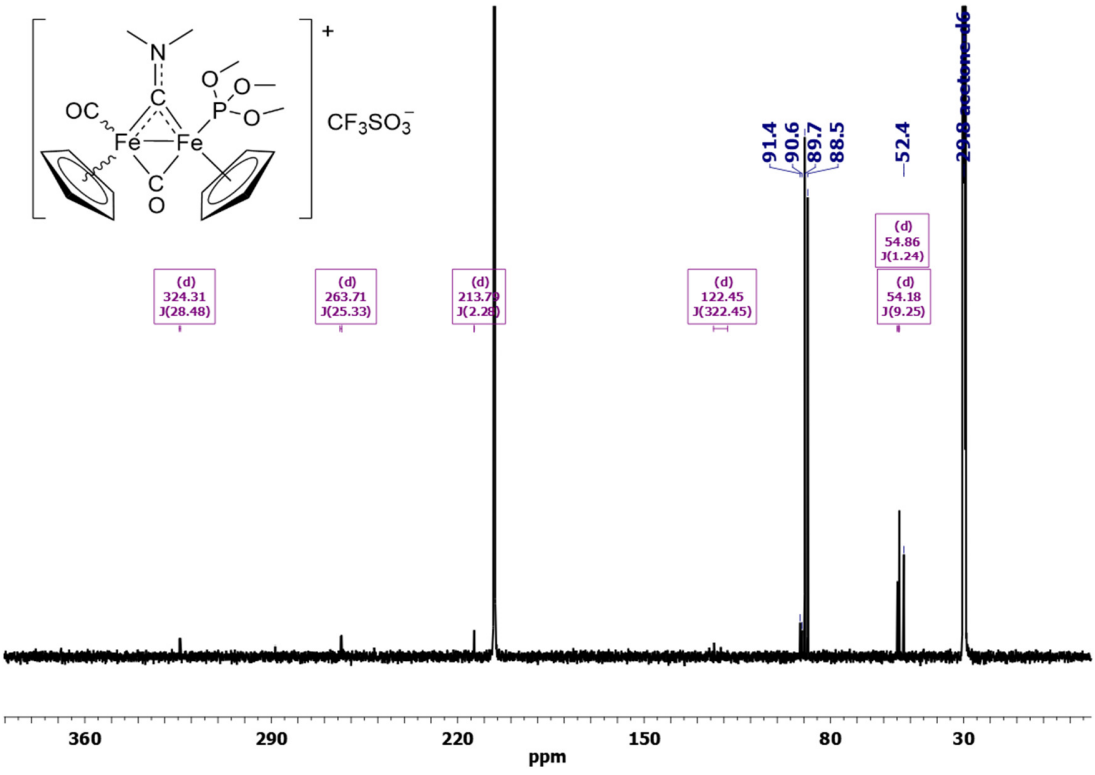

Figure S35. $^{31}P\{^{1}H\}$ NMR spectrum (162 MHz, acetone-d_6) of **3f** (*cis*/*trans* ratio ≈ 18).

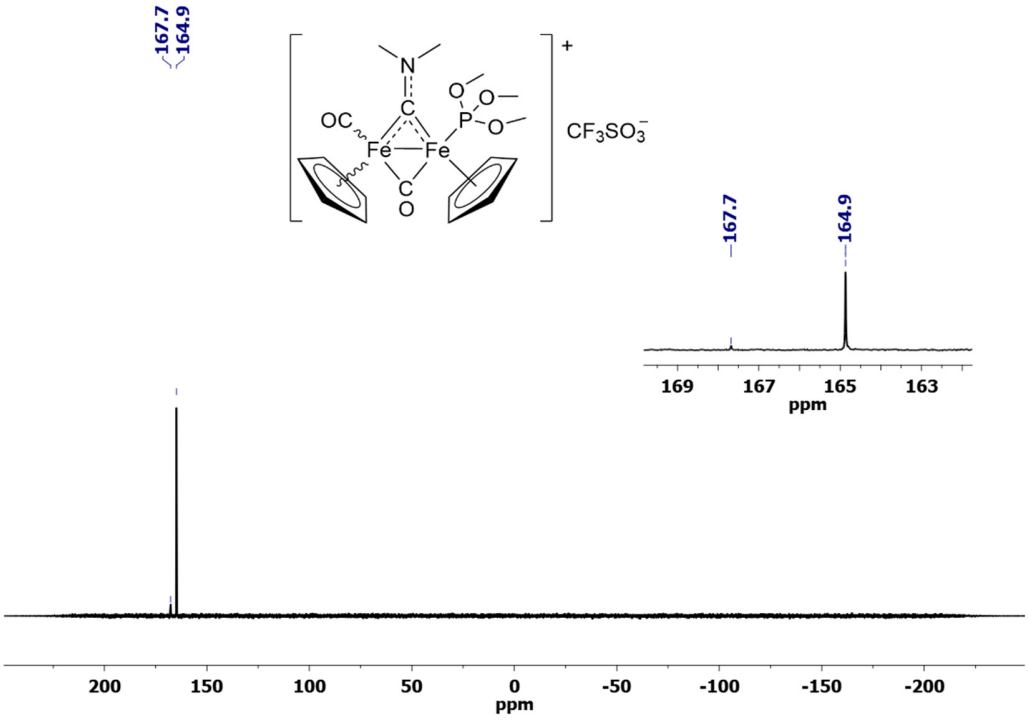

Figure S36. Black line: ^{1}H NMR spectrum (401 MHz, acetone-d_6) of *cis*-**3f**. Blue line: ^{1}H NOESY with irradiation at 5.14 ppm (Cp^{P}). Red line: ^{1}H NOESY with irradiation at 5.25 ppm (Cp). Observed NOEs are indicated by the arrows.

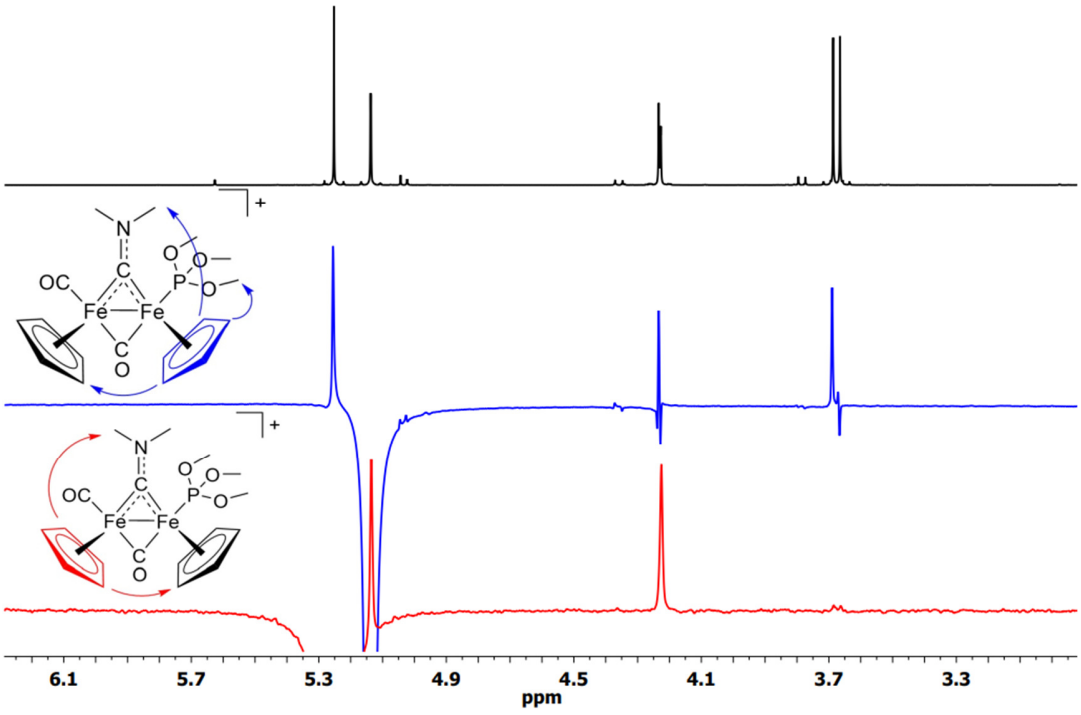

Figure S37. Solid-state IR spectrum (650-4000 cm^{-1}) of *cis*-$[Fe_2Cp_2(CO)(PPh_3)(\mu\text{-}CO)(\mu\text{-}CNMe_2)]CF_3SO_3$, **4f**.

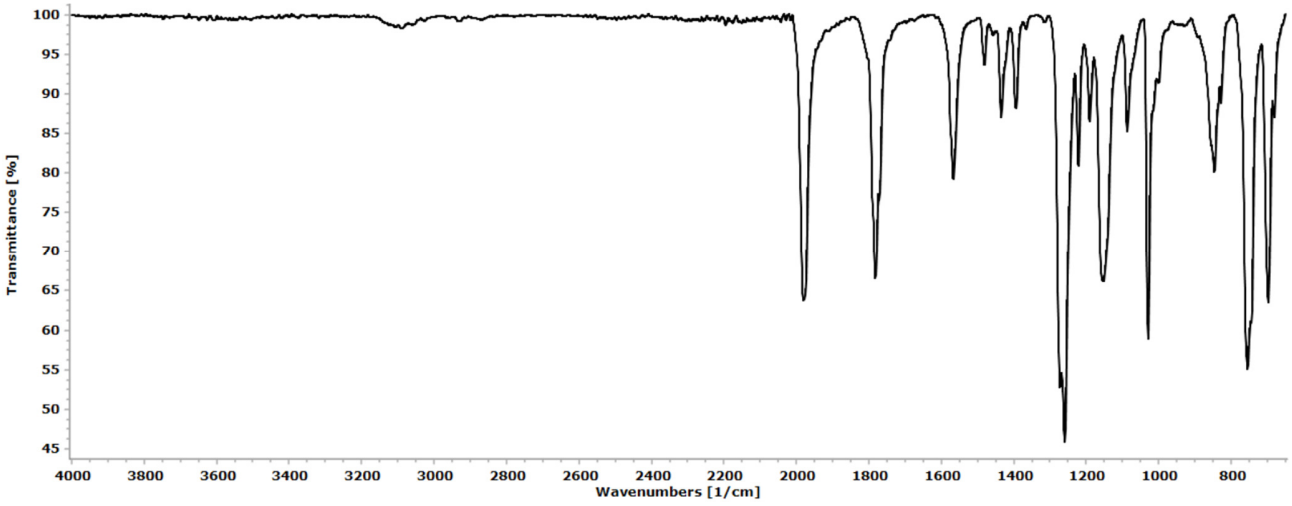

Figure S38. ^1H NMR spectrum (401 MHz, $CDCl_3$) of *cis*-**4f**.

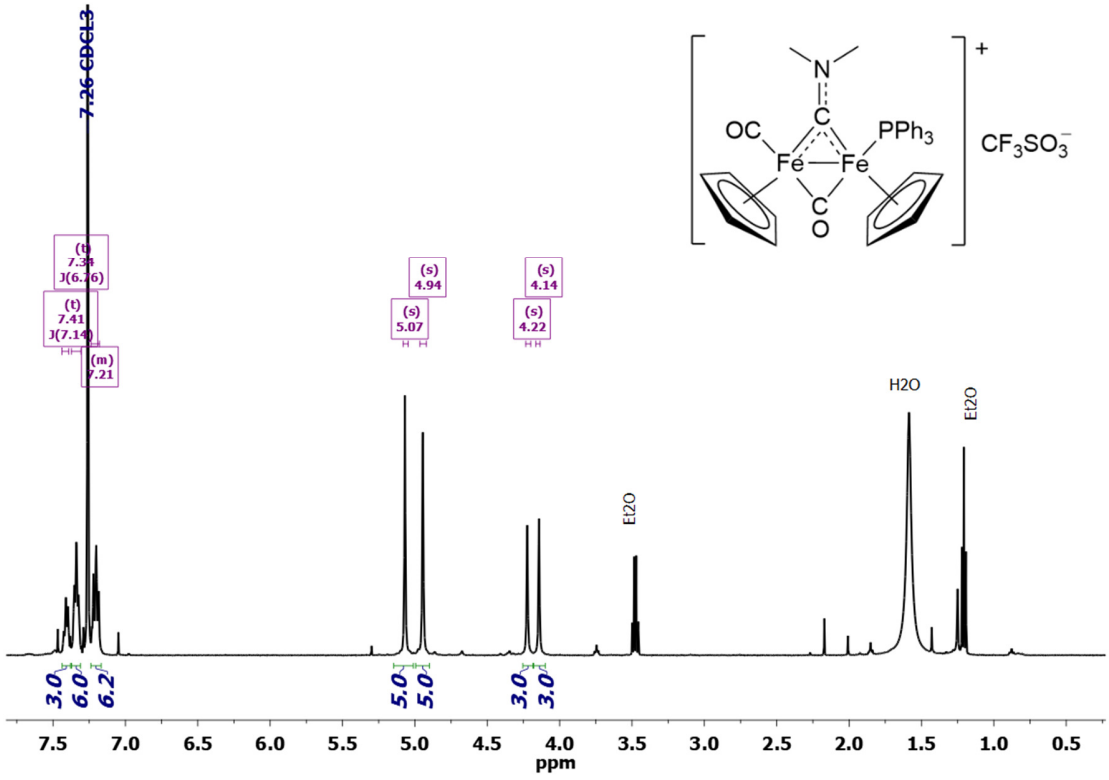

Figure S39. $^{31}P\{^{1}H\}$ NMR spectrum (162 MHz, $CDCl_3$) of *cis*-**4f**.

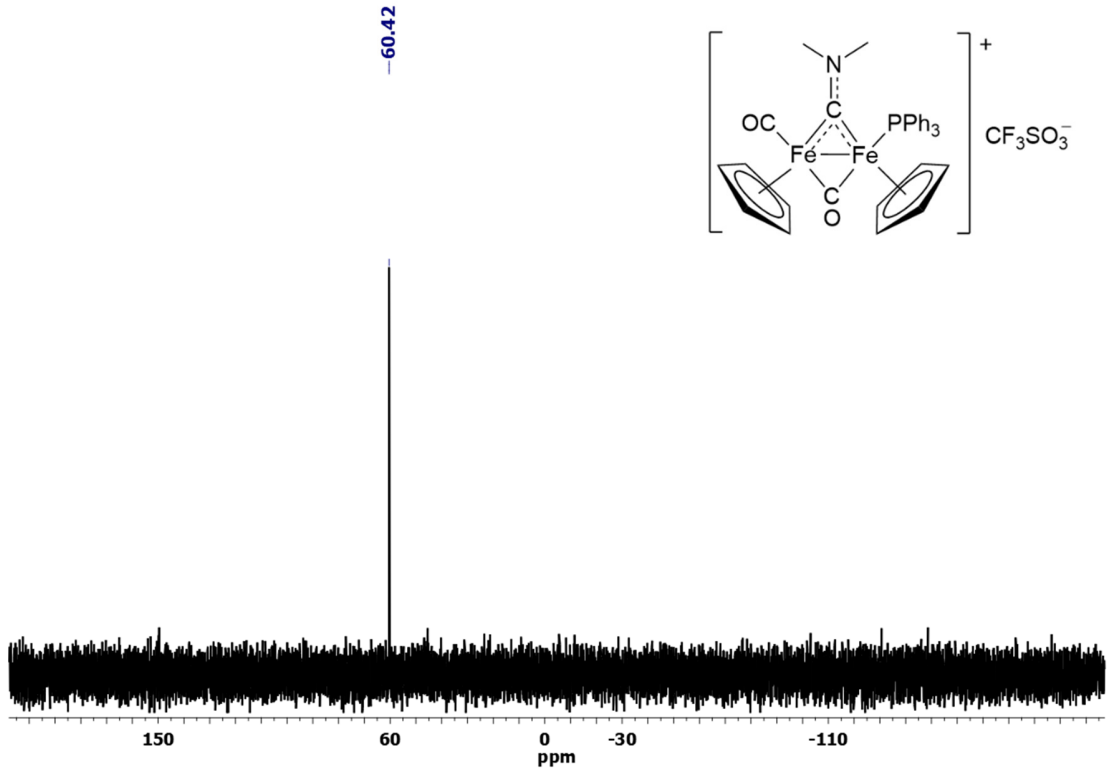

Figure S40. Solid-state IR spectrum (650-4000 cm^{-1}) of $[Fe_2Cp_2(CO)(PPh_2Me)(\mu\text{-}CO)(\mu\text{-}CNMe_2)]CF_3SO_3$, **5f** (*cis*/*trans* ratio ≈ 23).

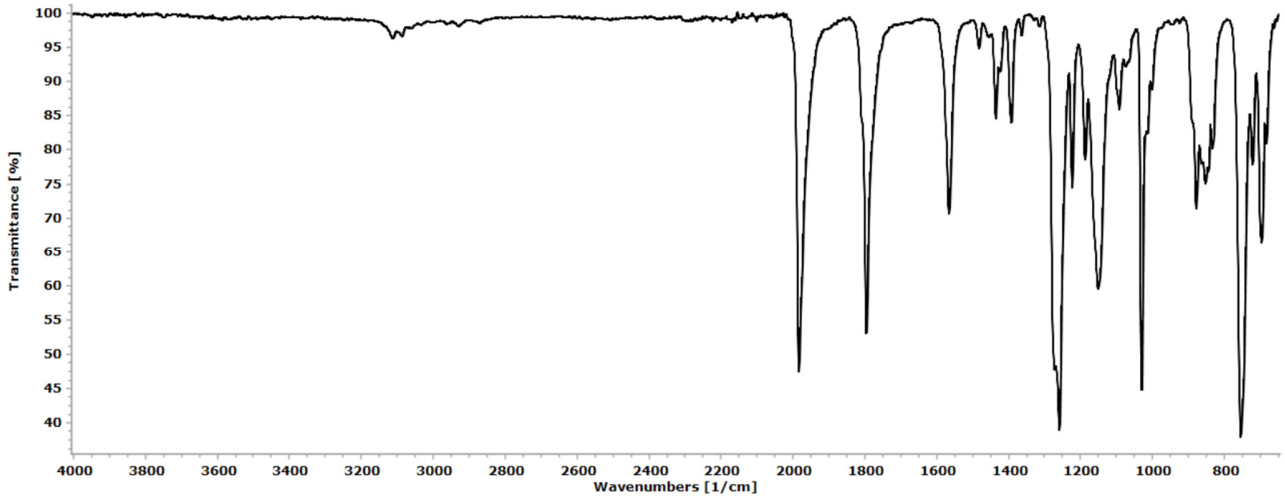

Figure S41. ^{1}H NMR spectrum (401 MHz, acetone-d_6) of **5f** (*cis*/*trans* ratio ≈ 23). Only resonances due to the *cis* isomer are integrated.

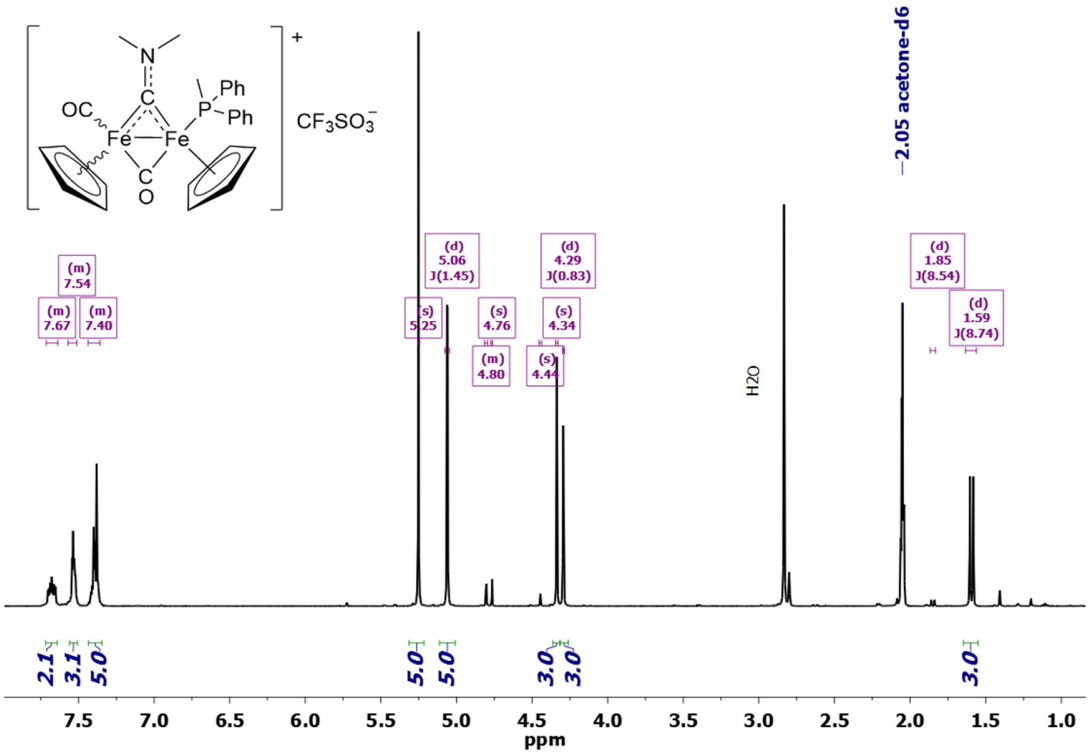

Figure S42. ^{13}C{^{1}H} NMR spectrum (101 MHz, acetone-d_6) of **5f** (*cis*/*trans* ratio ≈ 23).

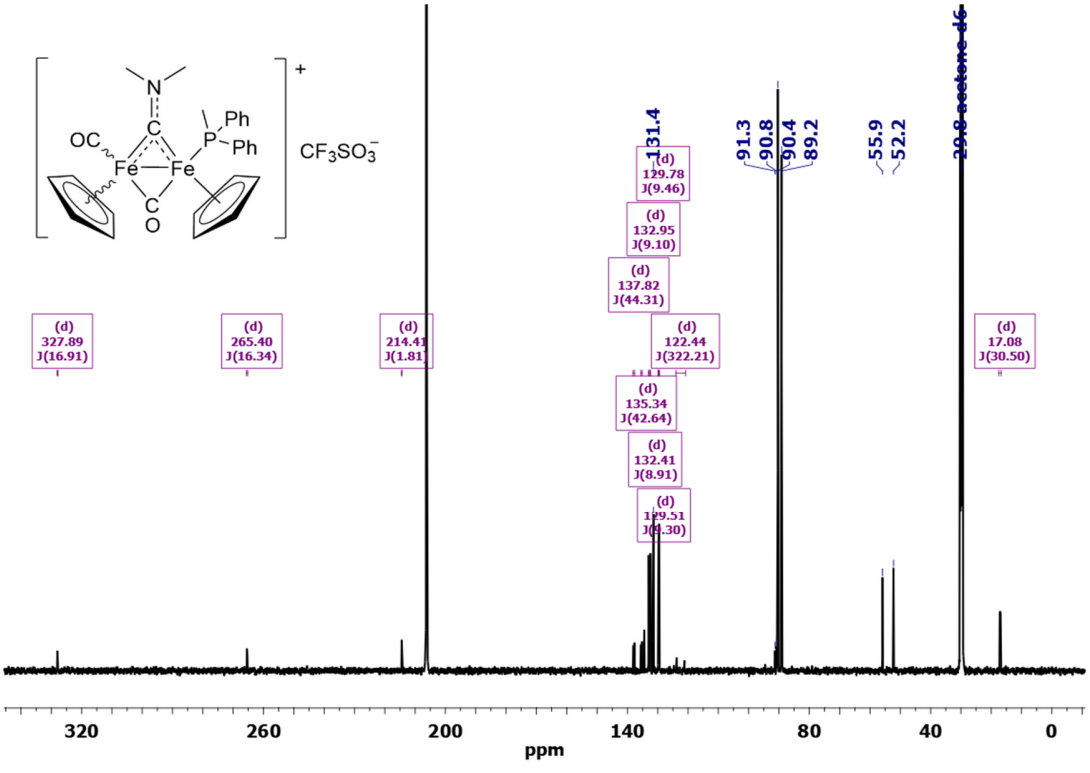

Figure S43. $^{31}P\{^{1}H\}$ NMR spectrum (162 MHz, acetone-d_6) of **5f** (*cis*/*trans* ratio ≈ 23).

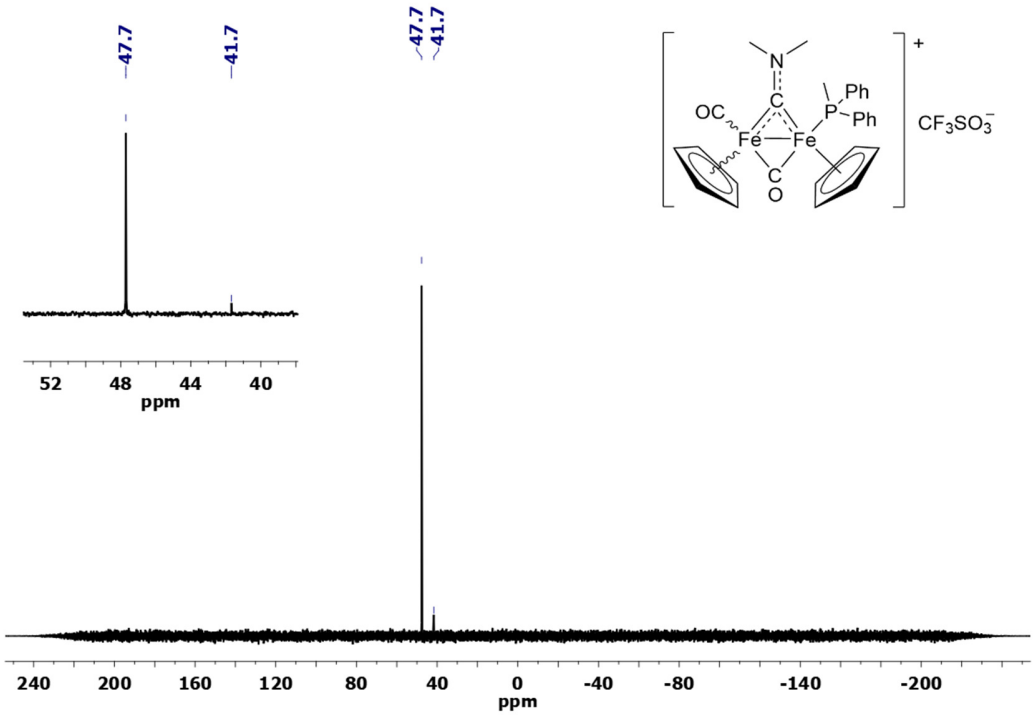

Figure S44. Black line: ^{1}H NMR spectrum (401 MHz, acetone-d_6) of *cis*-**5f**. Blue line: ^{1}H NOESY with irradiation at 5.06 ppm (Cp^{P}). Red line: ^{1}H NOESY with irradiation at 5.26 ppm (Cp). Observed NOEs are indicated by the arrows.

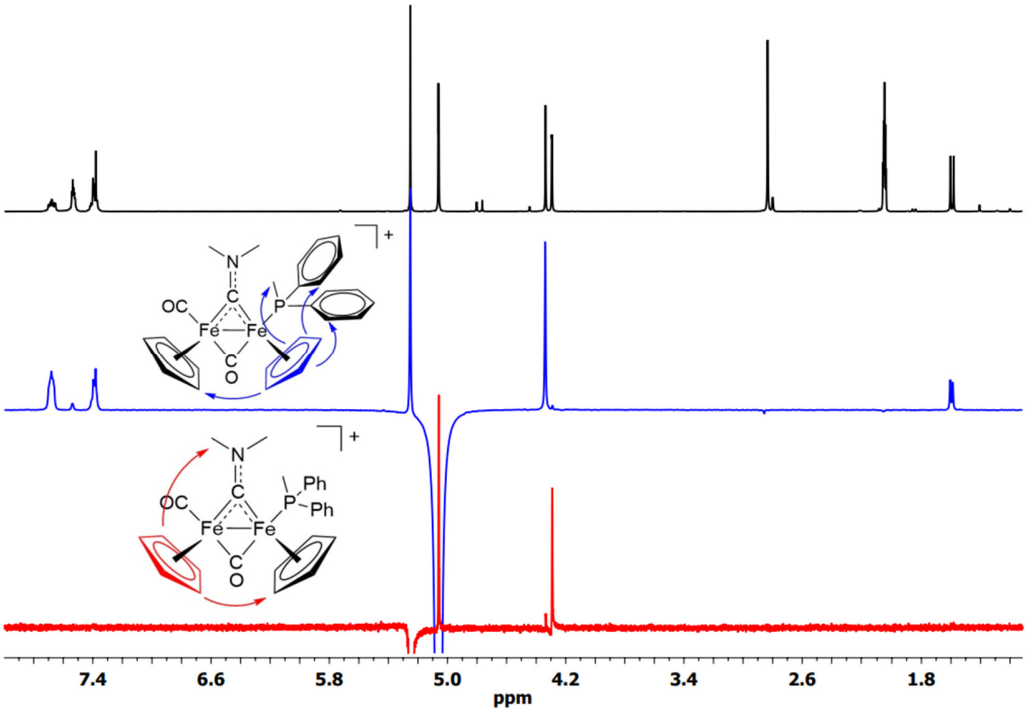

Figure S45. Flow injection ESI(+)-MS spectrum of **2a** in MeOH in the 100-1000 m/z range (below: zoom into the 572-586 m/z region).

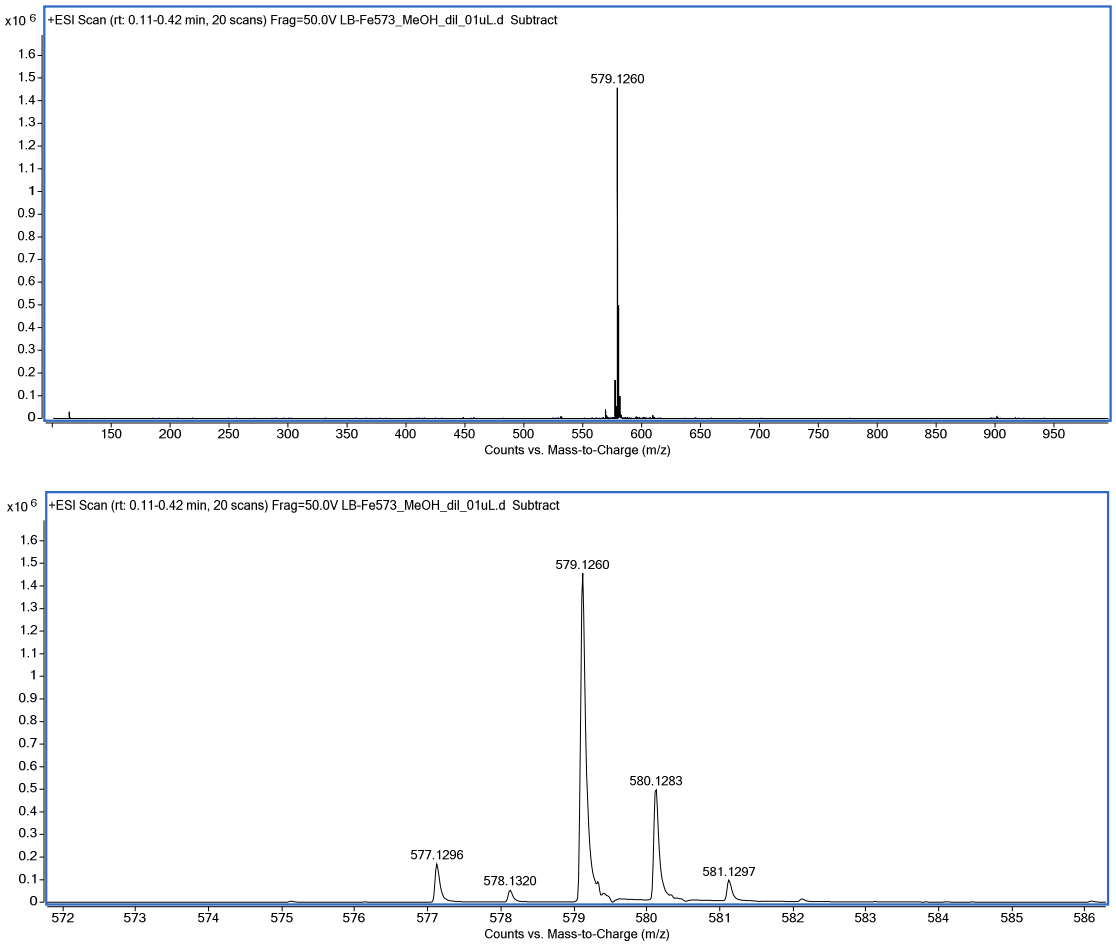

Figure S46. Flow injection ESI(+)-MS spectrum of **2a** in MeOH (black line) and calculated isotopic pattern (red boxes). Calcd. base peak for $C_{26}H_{36}Fe_2N_4O2P$: 579.1270 Da. Difference on the main peak (ppm): 1.9.

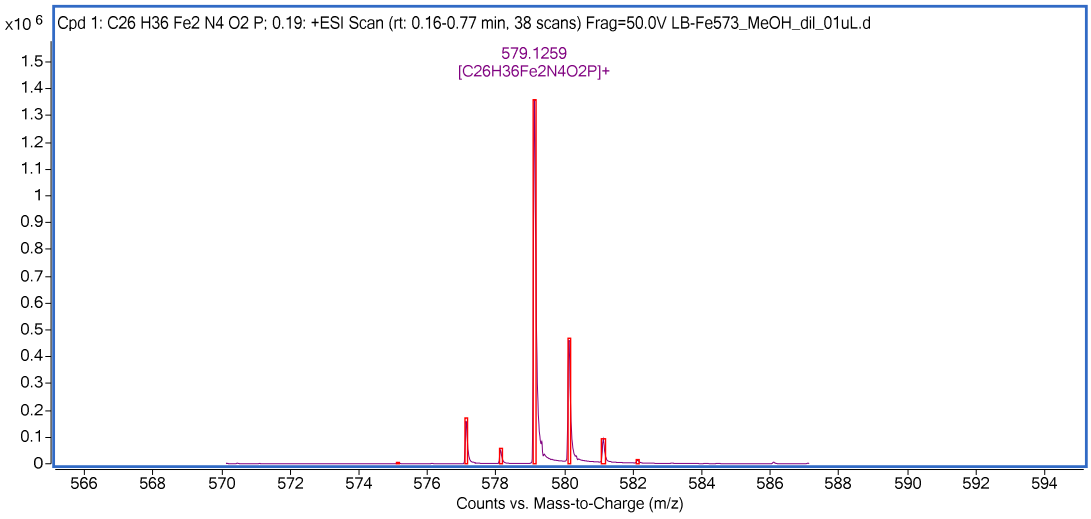

Thermal isomerization in isopropanol

Experimental procedure. A suspension of the selected diiron complex in ^{i}PrOH (3 mL) was stirred at reflux for 21 h then taken to dryness under vacuum. The resulting dark green-brown solid was analyzed by ^{1}H and ^{31}P NMR (acetone-d_6). **2a**: pure *E*-isomer (starting material); *cis*-*E*/*cis*-*Z* ratio = 4.5 (final product). **2e**: *cis*-*Z*/*cis*-*E* ratio (starting material) = 10; *cis*-*E*/*cis*-*Z* ratio = 20 (final product).

Figure S47. ^{31}P{^{1}H} NMR spectra (162 MHz, acetone-d_6) of **2a** before (top, dark blue line) and after (below, dark red line) treatment in refluxing ^{i}PrOH.

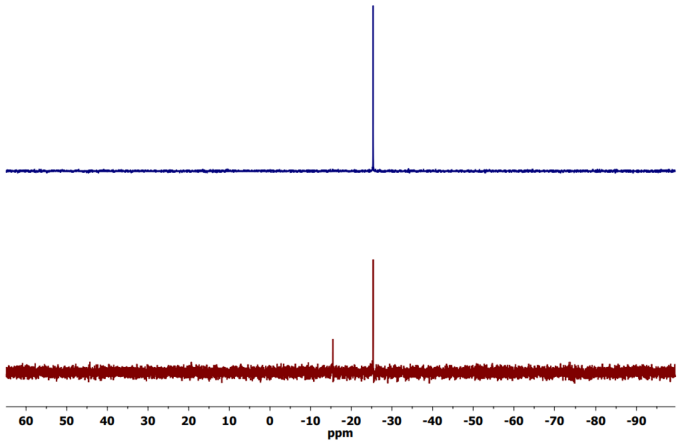

Figure S48. ^{1}H NMR spectrum (401 MHz, acetone-d_6) of **2a** after treatment in refluxing ^{i}PrOH (*cis*-*E*/*cis*-*Z* ratio 4.5). Resonances due to the *cis*-*E* isomer are highlighted.

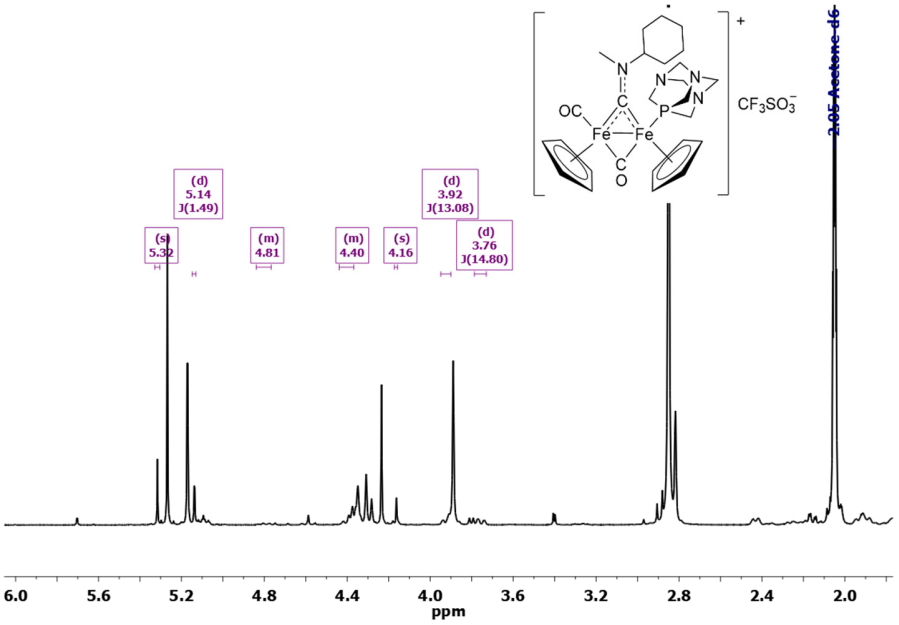

Figure S49. $^{31}P\{^{1}H\}$ NMR spectra (162 MHz, acetone-d_6) of **2e** before (top, dark blue line) and after (below, dark red line) treatment in refluxing ^{i}PrOH.

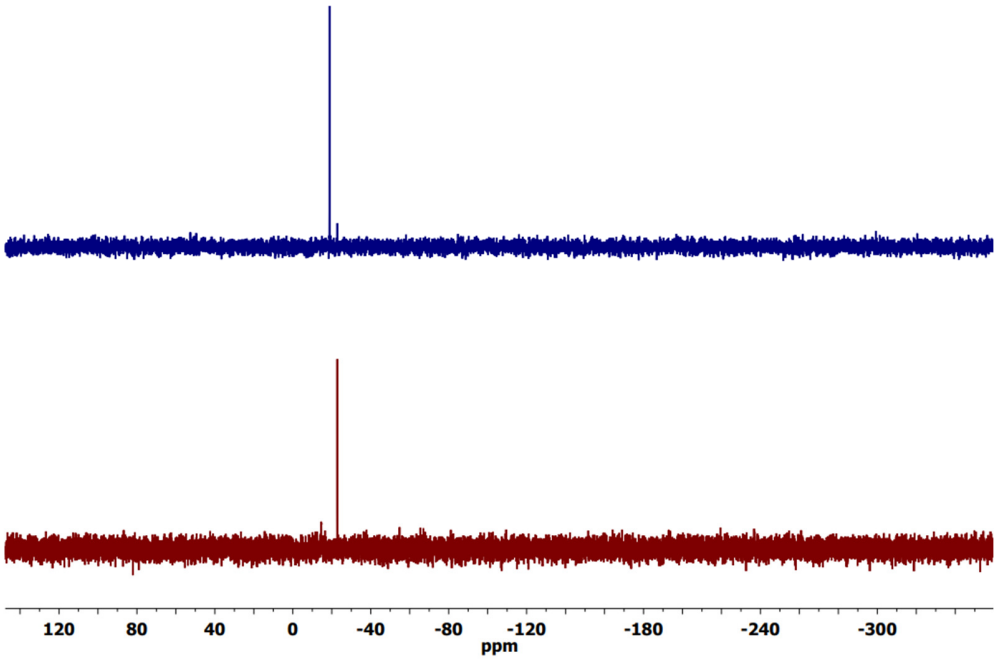

Figure S50. ^{1}H NMR spectrum (401 MHz, acetone-d_6) of **2e** after treatment in refluxing ^{i}PrOH (*cis-E*/*cis-Z* ratio 20). Resonances due to the *cis-E* isomer are highlighted.

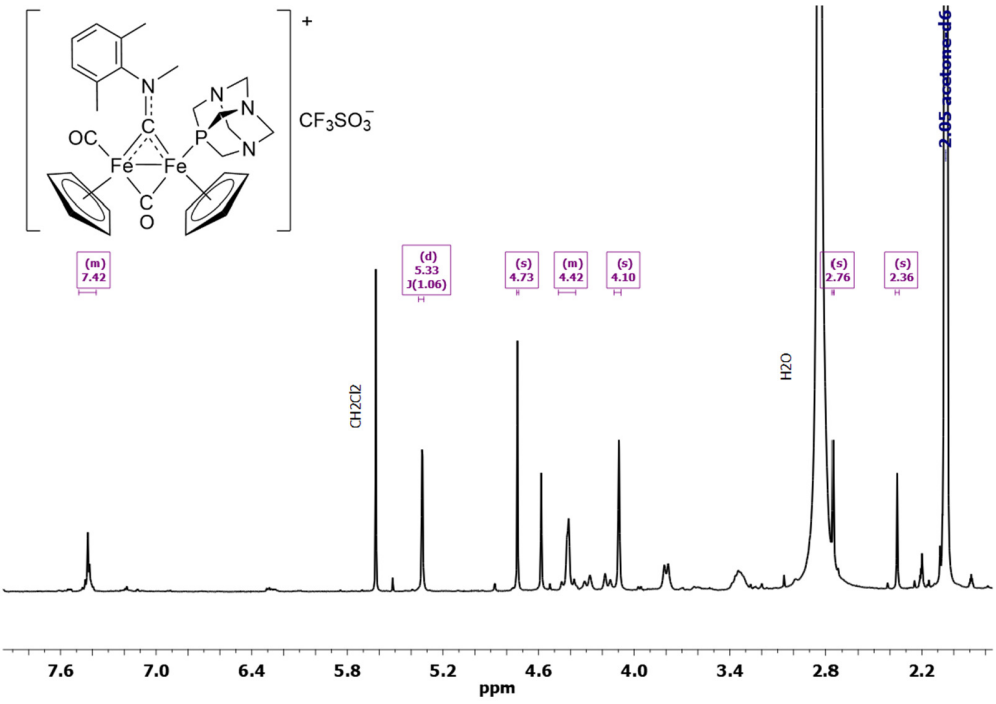

Table S1. Selected ^{13}C and ^{31}P NMR data for $[Fe_2Cp_2(CO)(PR_3)(\mu\text{-}CO)(\mu\text{-}CNR'R'')]CF_3SO_3$ complexes (PR_3 = PTA, **2a-f**; L = $P(OMe)_3$, **3c,f**; L = PPh_3, **4f**). Signals due to minor isomers are italicized.

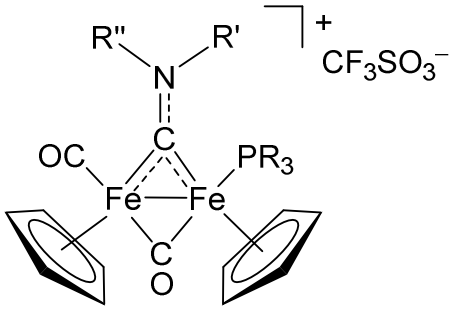

Complex	Aminocarbyne substituents (R', R'')	^{13}C NMR: δ / ppm [a]			^{31}P NMR: δ / ppm [a]	
		μ-CO	t-CO	μ-CN	*trans* / *cis-Z*	*cis* / *cis-E*
2a	Me, Cy	324.0	262.8	216.5	− *14.8*	− 24.7
2b	Me, *p*-C_6H_4OMe	331.5	262.4	217.0	− *14.6*	− 24.7
2c	Me, 2-naphthyl	331.4	262.2	217.0	− *14.4*	− 24.3
2d	Bn, Bn	330.9	262.6	216.9	− *18.1*	− 22.0
2e	Me, Xyl	331.5, *328.5*	*264.8*, 262.1	*215.5*, 214.6	− *17.0*	− 21.6
2f [b]	Me, Me	324.4	263.1	216.3	− *18.1*	− 22.0
3c	Me, 2-naphthyl	331.7	262.7	214.8, *213.9*	*166.3*, *163.7* [c]	164.1
3f	Me, Me	324.3	263.7	213.8	*167.7*	164.9
4f [d]		328.5	267.5	211.1	-	60.4
5f		327.9	265.4	214.4	*41.7*	47.7

[a] NMR data refer to acetone-d_6 solutions except for **2c** (DMSO-d_6) and **4f** ($CDCl_3$). [b] Data taken from the literature.[1] [c] *trans-E* isomer. [d] ^{13}C data taken from the literature.[2]

Table S2. Selected IR data for CH_2Cl_2 solutions of $[Fe_2Cp_2(CO)(L)(\mu\text{-}CO)(\mu\text{-}CNR'R'')]CF_3SO_3$ complexes (**L** = CO, **1a-f**; L = PTA, **2a-f**; L = $P(OMe)_3$, **3c,f**; L = PPh_3, **4f**, PPh_2Me, **5f**).

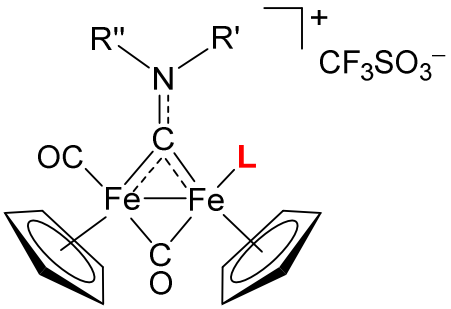

Complex	Aminocarbyne substituents (R', R'')	Ligand	IR: ũ / cm^{-1} [a]		
			ν(t-CO)	ν(μ-CO)	ν(μ-CN)
1a [b]	Me, Cy	CO	2020	1835	1567
2a		PTA	1965	1800	1533
		Δ (CO → PTA)	*− 55*	*− 35*	*− 34*
1b [b]	Me, *p*-C_6H_4OMe	CO	2021	1836	1540
2b		PTA	1963	1799	1519
		Δ (CO → PTA)	*− 58*	*− 37*	*− 21*
1c [b]	Me, 2-naphthyl	CO	2022	1837	1538
2c		PTA	1965	1801	1517
		Δ (CO → PTA)	*− 57*	*− 36*	*− 21*
3c			1986	1803	*1525*
		Δ (CO → P(OMe)$_3$)	*− 36*	*− 34*	*− 13*
1d [b]	Bn, Bn	CO	2023	1840	1550
2d		PTA	1968	1801	1514
		Δ (CO → PTA)	*− 55*	*− 39*	*− 36*
1e [b]	Me, Xyl	CO	2023	1840	1530
2e [c]		PTA	1978	1794	1505
		Δ (CO → PTA)	*− 45*	*− 46*	*− 25*
1f [b]	Me, Me	CO	2022	1835	1602
2f [b]		PTA	1967	1800	1573
		Δ (CO → PTA)	*− 55*	*− 35*	*− 29*
3f		$P(OMe)_3$	1987	1801	1584
		Δ (CO → P(OMe)$_3$)	*− 35*	*− 34*	*− 18*
4f		PPh_3	1986	1791	1570
		Δ (CO → PPh$_3$)	*− 36*	*− 44*	*− 32*
5f		PPh_2Me	1977	1793	1571
		Δ (CO → PPh$_2$Me)	*− 45*	*− 42*	*− 31*

[a] IR data refer to CH_2Cl_2 solutions. For **1a-f**, only the higher-energy stretching of terminal carbonyl ligands (t-CO) is considered. [b] Data taken from the literature.[1,3] [c] Refer to a *cis-Z*/*cis-E* 10:1 sample (*E*-rich mixtures display insufficient solubility in CH_2Cl_2).

Behavior of the diiron complexes in aqueous solutions

Solubility in water (D_2O). The selected compound was suspended in a D_2O solution (0.7 mL) containing dimethyl sulfone (Me_2SO_2; $4.5 \cdot 10^{-3}$ mol·L^{-1}) and stirred at room temperature (21 ± 1 °C) for 3 h. The saturated solution was filtered over celite and analyzed by ^{1}H NMR (delay time = 3 s; number of scans = 20). The concentration (= solubility) was calculated by the relative integral with respect to Me_2SO_2 as internal standard [δ/ppm = 3.14 (s, 6H)] (Table 1). NMR data are reported in the Supporting Information.

Octanol-water partition coefficient (Log P_{ow}). Partition coefficients (P_{ow}), defined as $P_{ow} = c_{org}/c_{aq}$, where c_{org} and c_{aq} are the molar concentrations of the selected compound in the n-octanol and aqueous phase, respectively, were determined by the shake-flask method and UV-Vis measurements, according to a previously described procedure.[4,5] All operations were carried out at room temperature (21±1 °C). Stock solutions were prepared in water-saturated octanol for all compounds except **2a,b** (in octanol-saturated water). The wavelength corresponding to a well-defined maximum of shoulder absorption of each compound (320–400 nm range) was used for UV-Vis quantitation. The procedure was repeated three times for each sample (from the same stock solution); results are given as mean ± standard deviation (Table 1).

Stability in water or water/methanol solutions. Compounds **2a-d** and **3f** were dissolved in a D_2O solution (0.7 mL) containing Me_2SO_2 ($4.5 \cdot 10^{-3}$ mol·L^{-1}). Alternatively, compounds **2e**, **3c** and **4-5f** were dissolved in CD_3OD (0.35 mL). then diluted with the D_2O/Me_2SO_2 solution (0.35 mL; 1:1 *v*/*v*). The final solution ($c_{Fe2} \approx 8 \cdot 10^{-3}$ mol·L^{-1}) was filtered over celite, analyzed by ^{1}H NMR (delay time = 3 s; number of scans = 20) and ^{31}P{^{1}H} NMR and subsequently heated at 37 °C for 72 h. After cooling to room temperature, the solutions were separated from a minor amount of red-brown precipitate by filtration over celite and NMR analyses was repeated. The residual amount of starting material in the final solution (with respect to the initial spectrum) was calculated by the relative integral with respect to Me_2SO_2 as

internal standard (Table 1). In each case, no new {FeCp} species was identified. NMR data are reported in the Supporting Information; ^{1}H NMR chemical shifts in D_2O/CD_3OD mixtures are referenced to the Me_2SO_2 peak in pure D_2O [δ/ppm = 3.14 (s, 6H)].

Stability in cell culture medium solution. Deuterated cell culture medium (DMEM-d) was prepared by dissolving powdered DMEM cell culture medium (1000 mg/L glucose and L-glutamine, without sodium bicarbonate and phenol red; D2902 - Merck) in D_2O (10 mg/mL, according to the manufacturer's instructions). The solution was treated with Me_2SO_2 (*ca*. $6\cdot10^{-3}$ mol·L^{-1}), NaH_2PO_4 and Na_2HPO_4 (25 mmol·L^{-1} total phosphate, pD = 7.4[6]), then stored under N_2. Solutions of Fe compounds in DMEM-d or in DMEM-d/CD_3OD mixtures were prepared, treated and analyzed as described above. The residual amount of starting material in solution after 24 h at 37 °C was calculated with respect to Me_2SO_2 as internal standard (Table 1).

NMR data and isomer ratios in aqueous solution.

^{1}H NMR chemical shifts are referred to dimethyl sulfone (Me_2SO_2) as in pure D_2O (δ_H = 3.14 ppm).

2a. Green-brown solution. ^{1}H NMR (D_2O): δ/ppm = *5.22*, 5.19 (s, 5H); 5.02, *4.99* (d, *J* = 1 Hz, 5H); 4.37, 4.26 (d, *J* = 13.1 Hz, 6H); 4.07, *4.02* (s, 3H); 4.03 (d, *J* = 10.4 Hz, 1H); *3.80*, *3.60* (d, *J* = 15 Hz), 3.74 (s) (6H); 2.29 (d, *J* = 12.2 Hz, 1H), 2.16–1.91 (m, 4H), 1.85–1.72 (m, 2H), 1.66–1.44 (m, 2H), 1.36–1.23 (m, 1H); *cis*-*E* isomer only (0 h), *cis*-*E*/*cis*-*Z* ratio = 2.8 (24-72 h).^{31}P{^{1}H} NMR (D_2O): δ/ppm = – *9.0*, –18.5.

2b. Green-brown solution. ^{1}H NMR (D_2O): δ/ppm = *7.79*, 7.58 (d, *J* = 8.5 Hz, 2H); *7.30*, 7.23 (d, *J* = 9.0 Hz, 2H); 5.11, *5.09* (d, *J* = 1.0 Hz, 5H); 4.64, *4.59* (s, 5H); 4.53, *4.50* (s, 3H); 4.42, 4.33 (d, *J* = 13.1 Hz, 6H); 3.93, 3.89 (s, 9H); isomer (*cis*-*E*/*cis*-*Z*) ratio *ca*. 15 (0 h), *ca*. 10 (72 h). ^{31}P{^{1}H} NMR (D_2O): δ/ppm = – *12.9*, – 18.0.

2c. Green-brown solution. ^{1}H NMR (D_2O): δ/ppm = 8.24 (d, *J* = 8.4 Hz), 8.16–8.07 (m) (4H); 7.78–7.68 (m, 3H); 5.16, *5.15* (s, 5H); 4.65 (s, 3H); *4.60*, 4.54 (s, 5H); 4.45, 4.37 (d, *J* = 13.7 Hz, 6H), 3.95 (s, 6H); isomer (*cis*-*E*/*cis*-*Z*) ratio = *ca*. 10 (0-72 h). ^{31}P{^{1}H} NMR (D_2O): δ/ppm = – *13.0*, – 17.9.

2d. Green-brown solution. ^{1}H NMR (D_2O): δ/ppm = 7.64, 7.55 (t, *J* = 7.1 Hz, 3H); 7.51–7.43 (m, 5H); 7.31–7.21 (m, 2H); 5.88, 5.76, 5.58, 5.38 (d, *J* = 14 Hz, 4H); 5.39, *5.27* (s, 5H); 5.01, *5.00* (d, *J* = 1.5 Hz, 5H); 4.35, 4.20 (d, *J* = 13.3 Hz, 6H); 3.69 (s-br, 6H); isomer (*cis*/*trans*) ratio = 15 (0-72 h). ^{31}P{^{1}H} NMR (D_2O): δ/ppm = – *13.5*, – 15.7.

2e. Green-brown solution. ^{1}H NMR (D_2O): δ/ppm = 7.50–7.33 (m, 3H); 5.39, *5.17* (s, 5H); 4.75, *4.67* (s,*); 4.41, 4.31 (d, *J* = 8.2 Hz), 4.40 (s) (9H); *3.94* (s), 3.68, 3.58 (d, *J* = 16.4 Hz) (6H); 2.69, *2.55* (s, 3H), 2.31, *2.28* (s, 3H); isomer (*cis*-*Z*/*cis*-*E*) ratio = 9, irrespective of the starting material. *Over HDO peak. ^{31}P{^{1}H} NMR (D_2O): δ/ppm = − 12.9, − *16.8*. ^{1}H NMR (D_2O/CD_3OD 1:1): δ/ppm = 7.53–7.36, *7.23–7.01* (m, 3H); 5.40, *5.17* (s, 5H); 4.75, *4.67* (s, 5H); 4.42, 4.31 (d, *J* = 13.7 Hz), 4.40 (s) (9 H); *3.94*

(s), 3.69, 3.59 (d, J = 15 Hz) (6H); 2.70, *2.66* (s, 3H); 2.32, *2.29* (s, 3H); isomer (*cis*-*Z*/*cis*-*E*) ratio: 4 (0 h); 0.55 (24 h); < 0.1 (72 h). $^{31}P\{^{1}H\}$ NMR (D_2O/CD_3OD 1:1): δ/ppm = − 12.9 (*Z*-**2e**), − 16.7 (*E*-**2e**).

3c. Red-brown solution. ^{1}H NMR (D_2O/CD_3OD 1:1): δ/ppm = 8.26 (d, J = 8.7 Hz), 8.14–8.01 (m) (4H); *7.86–7.78*, 7.77–7.66 (m, 3H); *5.31*, 5.20, *5.14* (s, 5H); 4.73, *4.59*, 4.57 (s, 3H); *4.55*, 4.53, *4.25* (s, 5H); *3.83*, 3.78, *3.62* (d, J = 11 Hz, 9H); isomer (*cis*-*E*/*trans*-*E*/*cis*-*Z*) ratio = 6.2:1.2:1 (0 h), 5:1:1 (72 h). $^{31}P\{^{1}H\}$ NMR (D_2O/CD_3OD 1:1): δ/ppm = *165.8*, 163.2, *162.8*.

3f. Orange-brown solution. ^{1}H NMR (D_2O): δ/ppm = 5.15, *4.98* (s, 5H); 5.04, *4.96* (s, 5H); 4.11, 4.10 (s, 6H); *3.68*, 3.61 (d, J = 10.8 Hz, 9H); isomer (*cis*/*trans*) ratio = 14 (0-72 h). $^{31}P\{^{1}H\}$ NMR (D_2O): δ/ppm = 164.3.

4f. Olive green-brown solution. ^{1}H NMR (D_2O/CD_3OD 1:1): δ/ppm = 7.54–7.48 (m, 3H), 7.46–7.40 (m, 6H), 7.28 (t, J = 8.9 Hz, 6H), 5.14 (s, 5H), 5.01 (s, 5H), 4.22 (s, 3H), 4.09 (s, 3H); *cis* isomer only. $^{31}P\{^{1}H\}$ NMR (D_2O/CD_3OD 1:1): δ/ppm = 60.0.

5f. Olive green-brown solution. ^{1}H NMR (D_2O/CD_3OD 1:1): δ/ppm = 7.66–7.52 (m, 6H); 7.45–7.35, 7.33–7.19 (m, 4H); 5.15 (s, 5H); 4.95* (s); 4.23, 4.18 (s, 6H); 1.57 (d, J = 8.7 Hz, 3H); isomer (*cis*/*trans*) ratio *ca*. 15 (0-72 h). *Covered by HDO resonance. $^{31}P\{^{1}H\}$ NMR (D_2O/CD_3OD 1:1): δ/ppm = 47.9.

Other species detected in solution.

O=PTA.[7] ^{1}H NMR (D_2O): δ/ppm = 4.03 (d, $^{2}J_{HP}$ = 10 Hz). $^{31}P\{^{1}H\}$ NMR (D_2O): δ/ppm = − 2.9.

O=P(OMe)$_3$.[8] ^{1}H NMR (D_2O): δ/ppm = 3.82 (d, $^{3}J_{HP}$ = 11 Hz). $^{31}P\{^{1}H\}$ NMR (D_2O): δ/ppm = 3.03.

O=PPh$_2$Me.[9] ^{1}H NMR (D_2O): δ/ppm = 2.16 (d, $^{2}J_{HP}$ = 12 Hz). $^{31}P\{^{1}H\}$ NMR (D_2O/CD_3OD 1:1): δ/ppm = 39.1.

Table S3. Comparison of water (D_2O) solubility and octanol/water partition coefficient (Log P_{ow}) for $[Fe_2Cp_2(CO)(L)(\mu\text{-}CO)(\mu\text{-}CNRR')]CF_3SO_3$ compounds (L = CO, **1a-f**; L = PTA, **2a-f**; L = $P(OMe)_3$, **3c,f**).

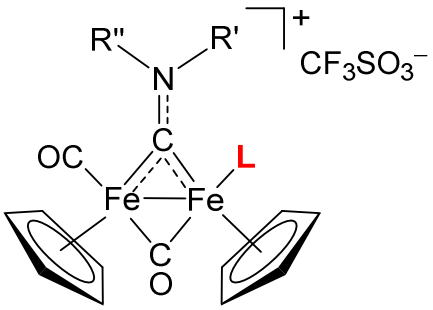

Aminocarbyne substituents (R', R'')		L = CO, 1a-f [a]		L = PTA, 2a-f [a][b]		L = $P(OMe)_3$, 3c,f [b]	
		D_2O solubility (mM)	Log P_{ow}	D_2O solubility (mM)	Log P_{ow}	D_2O solubility (mM)	Log P_{ow}
Me, Cy	**a**	6.2	− 0.46 ± 0.02	20	< − 1.5		
Me, *p*-C_6H_4OMe	**b**	4.1	− 0.25 ± 0.04	12	− 0.76 ± 0.01		
Me, 2-naphthyl	**c**	*not soluble* [c]	0.29 ± 0.03	1.8	− 0.04 ± 0.09	*not soluble* [c]	0.8 ± 0.1
Bn, Bn	**d**	0.6	0.2 ± 0.02	5.6	− 0.55 ± 0.05		
Me, Xyl	**e**	1.4	− 0.27 ± 0.04	1.1	− 0.74 ± 0.07		
Me, Me	**f**	3.2	− 0.9 ± 0.1	46	< − 2	4.1	− 0.75 ± 0.06

[a] Data for **1a-f** and **2f** is taken from the literature.[1,3] Solubility and Log_{10} P_{ow} of **2a** are related to the pure *cis-E* isomer. [b] Data is referred collectively to all isomers present in solution, except for **2-3f** (single *cis*- isomer). [c] Below the lowest value of quantitation (*ca*. $3 \cdot 10^{-4}$ M).

Table S4. Comparison of thermal stability (% residual complex) at 37 °C in water and cell culture medium for $[Fe_2Cp_2(CO)(L)(\mu\text{-}CO)(\mu\text{-}CNRR')]CF_3SO_3$ compounds (L = CO, **1a-f**; L = PTA, **2a-f**; L = $P(OMe)_3$, **3c,f**).

		% residual complex (37 °C, ^1H NMR) [a]					
Aminocarbyne Substituents (R', R'')		L = CO, 1a-f [b]		L = PTA, 2a-f [b][c]		L = $P(OMe)_3$, 3c,f [c]	
		D_2O ± CD_3OD 72 h	DMEM-d ± CD_3OD 24 h	D_2O ± CD_3OD 72 h	DMEM-d ± CD_3OD 24 h	D_2O ± CD_3OD 72 h	DMEM-d ± CD_3OD 24 h
Me, Cy	**a**	75	85	90	90		
Me, *p*-C_6H_4OMe	**b**	86	77	88	90		
Me, 2-naphthyl	**c**	66 [d]	*n.p.*	61	91	79 [d]	93 [d]
Bn, Bn	**d**	≈ 50	75	78	91		
Me, Xyl	**e**	79	70	81 [d]	91 [d]		
Me, Me	**f**	70	76	70	*n.p.*	73	85

[a] Experiments were carried out in aqueous solution (D_2O or DMEM-d) except where otherwise noted. [b] Data for **1a-d,f** and **2f** is taken from the literature.[1,3] Data for **1e** is new (re-determined with respect to the literature). [c] Data is referred collectively to all isomers present in solution, except for **2-3f** (single *cis*- isomer). [d] In deuterated water/methanol 1:1 *v*/*v* mixtures. *n.p.* = not performed.

Table S5. Isomer ratios for $[Fe_2Cp_2(CO)(PR_3)(\mu\text{-}CO)(\mu\text{-}CNR'R'')]CF_3SO_3$ complexes **2-5** in organic (acetone-d_6) or aqueous (D_2O, DMEM-d and their mixtures with CD_3OD mixtures) solutions. Wavy bonds refer to *cis*/*trans* and *E*/*Z* isomerism.

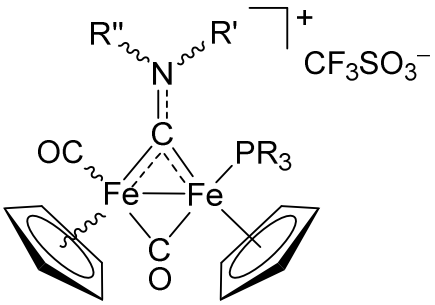

Complex	Isomers observed (major first)	Isomer ratio (^{1}H NMR)		
		Acetone-d_6 Freshly prepared	D_2O/DMEM-d ± CD_3OD [a]	
			Freshly prepared	37 °C, 72 h
2a	*cis-E*, *cis-Z*	- (only *cis-E*) [b]	- (only *cis-E*)	2.8
2b	*cis-E*, *cis-Z*	20	15	10
2c	*cis-E*, *cis-Z*	7	10	10
2d	*cis*, *trans*	15	15	15
2e	*cis-Z*, *cis-E*	4 [d]	9 (D_2O); 4	< 0.1
2f [c]	*cis, trans*	- (only *cis*) [b]	- (only *cis*)	- (only *cis*)
3c	*cis-E, trans-E, cis-Z*	13:1.6:1	6.2:1.2:1	5:1:1
3f	*cis*, *trans*	18	14	14
4f	*cis*	- (only *cis*) [e]	- (only *cis*)	- (only *cis*)
5f	*cis*, *trans*	23	15	15

[a] Experiments for **2a-d,f** and **3f** were carried out in aqueous solution (D_2O or DMEM-d); for **2e**, **3c**, **4f**, **5f** in 1:1 *v*/*v* mixtures of deuterated water/methanol. [b] Pure isomer isolated from a raw *cis-E*/*cis-Z* (**2a**) or *cis*/*trans* (**2f**) mixture. [c] Data taken from the literature.[1] [d] Mixtures with different isomer ratios can be obtained according to the synthetic procedure. [e] in $CDCl_3$.

Cyclic Voltammetry

Cyclic voltammetry measurements were performed at room temperature with a PalmSens4 instrument and PSTrace5 software. Phosphate buffer saline solution (NaCl 0.137 mol/L; Na_2HPO_4/KH_2PO_4, $c_{phosphate}$ = 27 mM, pH = 7.2) prepared in ultrapure H_2O was used as supporting electrolyte. The electrochemical cell was equipped with a Pt wire counter electrode, teflon-encapsulated glassy-carbon (GC) working electrode (eDAQ, ø 1 mm) and leak-free Ag/AgCl/KCl 3.4 mol/L reference electrode (eDAQ; E° = +0.205 V *vs* NHE).[10] Prior to measurements, the GC electrode was polished by manual rubbing with 0.3 µM Al_2O_3 slurry in water (eDAQ) for 2 min, sonication in ultrapure water for 10 min, manual rubbing with 0.05 µM Al_2O_3 slurry in water (eDAQ) for 2 min, sonication in ultrapure water for 10 min.[11] The supporting electrolyte (5.0 mL) was introduced into the cell and deaerated by Ar bubbling for some minutes. The working electrode was cycled several times between cathodic and anodic limits (–1.295 V to +1.605 V) until there was no change in the charging current. Compound **2a** was then introduced (c = $6 \cdot 10^{-4}$ mol/L) and voltammograms were recorded (Figure S51). Potentials are reported *vs*. NHE. Current sign convention: negative currents/cathodic process; positive currents/anodic process.

Figure S51. Cyclic voltammogram of **2a** ($6 \cdot 10^{-4}$ mol/L) recorded at a glassy carbon electrode in phosphate buffer saline solution (pH = 7.2). Scan rate: 100 mV/s. Arrows indicate scan direction.

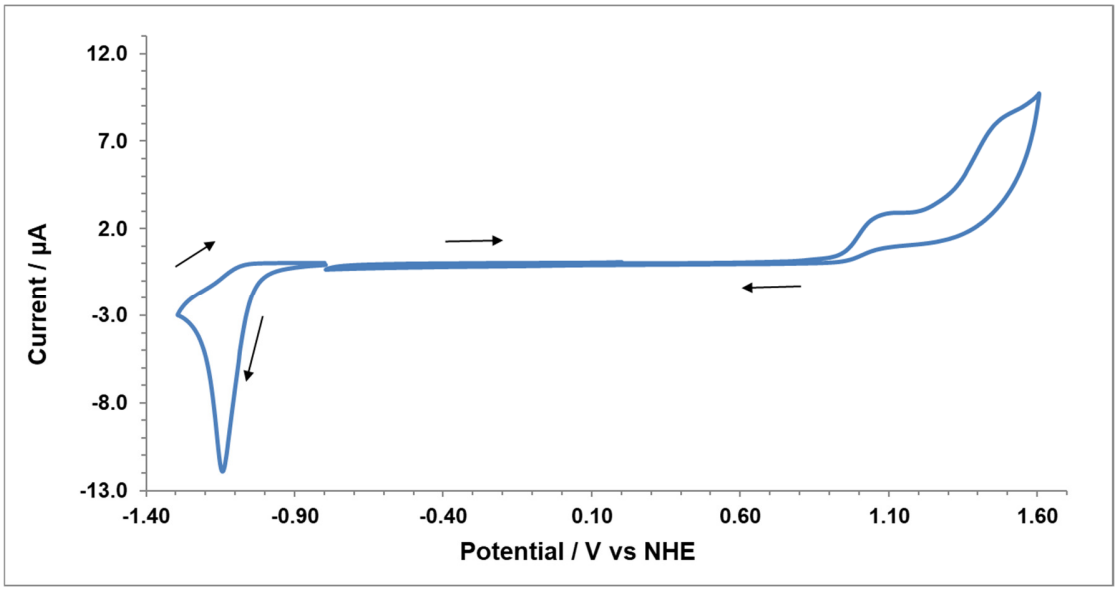

X-Ray crystallography

Crystal data and collection details for **2d**·solv and **3f** are reported in Table S6. Data were recorded on a Bruker APEX II diffractometer equipped with a PHOTON2 detector using Mo–Kα radiation. Data were corrected for Lorentz polarization and absorption effects (empirical absorption correction SADABS).[12] The structures were solved by direct methods and refined by full-matrix least-squares based on all data using F^2.[13] Hydrogen atoms were fixed at calculated positions and refined by a riding model. All non-hydrogen atoms were refined with anisotropic displacement parameters. The unit cell of **2d**·solv contains an additional total potential solvent accessible void of 230 Å^3 (*ca*. 6.3% of the Cell Volume), which is likely to be occupied by further highly disordered CH_3CN molecules. These voids have been treated using the SQUEEZE routine of PLATON.[14, 15]

Table S6. Crystal data and measurement details for **2d**·solv and **3f**.

	2d·solv	**3f**
Formula	$C_{34}H_{36}F_3Fe_2N_4O_5PS$	$C_{19}H_{25}F_3Fe_2NO_8PS$
FW	812.40	627.13
T, K	291(2)	100(2)
λ, Å	0.71073	0.71073
Crystal system	Monoclinic	Monoclinic
Space group	$P2_1/c$	Cc
a, Å	12.3463(8)	18.7231(7)
b, Å	14.3108(9)	8.4807(3)
c, Å	21.1212(12)	15.2741(6)
β,°	102.900(2)	97.2840(10)
Cell Volume, Å^3	3637.6(4)	2405.73(16)
Z	4	4
D_c, g·cm^{-3}	1.483	1.731
μ, mm^{-1}	0.960	1.428
F(000)	1672	1280
Crystal size, mm	0.21×0.17×0.16	0.22×0.21×0.18
θ limits,°	1.962–26.000	2.193–27.000
Reflections collected	39646	17893
Independent reflections	7121 [R_{int} = 0.0551]	5207 [R_{int} = 0.0271]
Data / restraints /parameters	7121 / 18 / 451	5207 / 2 / 322
Goodness on fit on F^2	1.171	1.063
R_1 ($I > 2\sigma(I)$)	0.0692	0.0183
wR_2 (all data)	0.1609	0.0455
Largest diff. peak and hole, e Å^{-3}	1.169 / –0.527	0.279 / –0.233

In vivo biological studies

All studies involving animal testing were carried out acknowledging the European Directive 2010/63/UE as to the animal welfare and protection and the related codes of practice (Italian Ministry of Health - 640/2016-PR). The mice were purchased from Charles River, housed in steel cages under controlled environmental conditions (constant temperature, humidity, and 12 h dark/light cycle), and alimented with commercial standard feed and tap water ad libitum. The Lewis lung carcinoma (LLC) cell line was purchased from ECACC, UK. The LLC cell line was maintained in D-MEM (Euroclone) supplemented with 10% heat-inactivated FBS (Euroclone), 10 mM L-glutamine, 100 U mL^{-1} penicillin, and 100 µg mL^{-1} streptomycin in a 5% CO_2 air incubator at 37 °C.

Wildtype, female C57BL/6 mice (6–8 weeks, 24±3 g body weight) were injected in the right flank with LLC (2×10^6 cells) and allowed to grow for 7 days (visible tumor), then randomized into treatment groups (5 animals per group, 8 controls). Mice were then treated for 5 days with cisplatin (3 mg/kg i.p.), or complex **2a** (8 mg/kg i.p.) or vehicle (saline solution). Chemotherapy doses were based on preliminary experiments to determine the maximum tolerated dose that did not induce excess weight loss or toxicity. At day 15 animals were sacrificed, the legs were amputated at the proximal end of the femur, and the inhibition of tumor growth was determined according to the difference in weight of the tumor-bearing leg and the healthy leg of the animals expressed as % referred to the control animals.

Body weight was measured at day 1 and every two days from day 7. Mice treated with the iron complexes showed no anorexia or other signs of systemic toxicity, whereas those treated with the reference platinum-based drug appeared prostrate and showed substantial weight loss. All the values are the means ± S.D. of not less than three measurements. $^{**}p < 0.01$; $^{*}p < 0.05$).

Notes and references

1 Agonigi, G.; Biancalana, L.; Lupo, M. G.; Montopoli, M.; Ferri, N.; Zacchini, S.; Binacchi, F.; Biver, T.; Campanella, B.; Pampaloni, G.; Zanotti, V.; Marchetti, F. *Organometallics* **2020**, *39*, 645-657.

2 Albano, V. G.; Busetto, L.; Marchetti, F.; Monari, M.; Zacchini, S.; Zanotti, V. Synthesis and Characterization of New Diiron and Diruthenium μ-Aminocarbyne Complexes Containing Terminal S-, P- and C-Ligands, *Z. Naturforsch*. **2007**, *62b*, 427–438.

3 Biancalana, L.; De Franco, M.; Ciancaleoni, G.; Zacchini, S.; Pampaloni, G.; Gandin, V.; Marchetti, F. Easily Available, Amphiphilic Diiron Cyclopentadienyl Complexes Exhibit in Vitro Anticancer Activity in 2D and 3D Human Cancer Cells through Redox Modulation Triggered by CO Release, *Chem. Eur. J.* **2021**, *27*, 10169-10185.

4 OECD Guidelines for Testing of Chemicals. In OECD, Paris: 1995; Vol. 107.

5 Dearden, J. C.; Bresnen, G. M. *Quant. Struct.-Act. Relat.* **1988**, *7*, 133-144.

6 Calculated by the formula pD = pH* + 0.4, where pH* is the value measured for H_2O-calibrated pH-meter; (a) Westcott, C. C. pH Measurements; Academic Press: New York, **1978**; (b) Covington, A. K.; Paabo, M.; Robinson, R. A.; Bates, R. G. *Anal. Chem.* **1968**, *40*, 700-706.

7 Daigle, D. J.; Decuir, T. J.; Robertson, J. B.; Darensbourg, D. J. 1,3,5-Triaz-7-Phosphatricyclo[3.3.1.13,7]Decane and Derivatives, *Inorganic Syntheses* **1998**, *32*, 40-45.

8 Meng, Q.; Doetschman, D. C.; Rizos, A. K.; Lee, M.-H.; Schulte, J. T.; Spyros, A.; Kanyi, C. W. Adsorption of Organophosphates into Microporous and Mesoporous NaX Zeolites and Subsequent Chemistry, *Environ. Sci. Technol*. **2011**, *45*, 3000-3005.

9 Renard, P.-Y.; Vayron, P.; Leclerc, E.; Valleix, A.; Mioskowski, C. Lewis Acid Catalyzed Room-Temperature Michaelis–Arbuzov Rearrangement, Angew. Chem. Int. Ed. 2003, 115, 2491-2494.

10 "Electrochemistry for Chemists, Second Edition", Sawyer, D. T.; Sobkowiak, A. J.; Roberts Jr., J. John Wiley & Sons, NY (**1995**). See Section 5.2.

11 Gross, M.; Jordan, J.; Voltammetry At Glassy Carbon Electrodes, *Pure & Appl. Chem*. **1984**, *56*, 1095-1129.

12 Sheldrick, G. M. SADABS-2008/1 - Bruker AXS Area Detector Scaling and Absorption Correction, Bruker AXS: Madison, Wisconsin, USA, **2008**.

13 Sheldrick, G. M. Crystal structure refinement with SHELXL. *Acta Cryst. C* **2015**, *71*, 3.

14 Spek, A. L. Single-crystal structure validation with the program PLATON, *J. Appl. Cryst*. **2003**, *36*, 7-13.

15 Spek, A. L. Structure validation in chemical crystallography, *Acta Cryst.* **2009**, *D65*, 148-155.